FRONTIERS OF BIOGEOGRAPHY
The scientific journal of The International Biogeography Society

Frontiers of Biogeography 19, 2026, e181379 | DOI 10.21425/fob.19.181379

RESEARCH ARTICLE

Climatic swings triggered incipient postglacial speciation of flightless *Calosoma* beetles in Western Balkan sky islands

Cody Raul Cardenas[1], Jérémy Gauthier[1,2], Hélène Mottaz[1], Julia Bilat[1], Slavčo Hristovski[3], Emmanuel F. A. Toussaint[1]

1 *Natural History Museum of Geneva, Geneva, Switzerland*
2 *Naturéum - State Museum of Natural Sciences, Lausanne, Switzerland*
3 *Institute of Biology, Faculty of Natural Sciences and Mathematics, Ss. Cyril and Methodius University, Skopje, Republic of North Macedonia*

Corresponding authors: Cody Raul Cardenas (cody-raul.cardenas@geneve.ch, nepenthesbaphomet@outlook.com); Emmanuel F. A. Toussaint (emmanuel.toussaint@geneve.ch)

Editor Xiaolei Huang
Received 31 December 2025 ♦ **Accepted** 6 April 2026 ♦ **Published** 18 May 2026

Abstract

Climatic change drastically shapes the ecology and evolution of lineages across landscapes. In mountainous regions, climatic oscillations drive fine-scale biome shifts and modulate habitat availability along elevation gradients, thereby governing population connectivity. Cold-adapted highland lineages with low dispersal capacity are ideal systems for studying the impact of past climates on geographic range shifts and genomic signatures. Here, we focus on the flightless highland species *Calosoma* (*Callisthenes*) *pentheri* endemic to the Western Balkan mountains, which exhibits a disjunct geographic distribution. We predict that glacial and interglacial periods drove allopatry through cycles of isolation and secondary contact, leaving genomic signatures among populations. Using hyRAD museomics combined with a newly sequenced reference genome we generated 10,794 single nucleotide polymorphisms and 2,278 loci to reconstruct the evolutionary history of this lineage. Admixture and phylogenomic analyses demonstrate clear delineation between the two lineages reflecting their distribution across the Western Balkans. Genetic signatures and divergence-time estimates suggest that these two lineages represent distinct species that diverged in the Late Miocene with little interspecific, but occasional intraspecific, admixture since the Pliocene. The diversification of these species in the Balkans was likely driven by isolation in sky island glacial refugia during the Miocene to Pliocene. Subsequent secondary contact during Pleistocene glacial periods may have occurred but did not result in introgression. Climatic oscillations during Quaternary ice ages similarly triggered admixture between populations of each massif. These species display intermediate stages along the speciation continuum, representing a model system for in-depth studies of climate-driven evolution in sky islands.

Highlights

- Genome-wide data generated from across the range of the Western Balkan highland endemic beetle *Calosoma pentheri* support the recognition of two distinct species.
- Divergence between these two species predates Quaternary glaciations and was shaped by Late Miocene to Pliocene climatic swings.
- Repeated cycles of isolation and connectivity across mountain reliefs have left a distinctive genomic signature among populations.
- Natural history collection specimens provide robust genomic data for phylogeographic analyses.
- Western Balkan sky islands exemplify how past climatic oscillations fostered lineage diversification, with current global warming trends threatening these unique ecosystems.

Keywords

Balkan Phylogeography, Beetle evolution, Carabidae genomics, Coleoptera, Mountain biogeography, Museomics, Population genomics

Introduction

Understanding the impact of climate change on biodiversity is one of the most pressing challenges in biology (Araújo and Rahbek 2006; Dawson et al. 2011; Bellard et al. 2012; Malinsky et al. 2021; Wiens and Zelinka 2024). With increasing global temperatures, biome shifts and drastic ecosystem reconfigurations are unfolding (Grimm et al. 2013; Scheffers et al. 2016; Freeman et al. 2018; Hughes et al. 2018). To better appreciate the resilience of biodiversity to such changes, one can look to the past to gain insight into possible future outcomes (Willis et al. 2010; Barnosky et al. 2017). Periods of comparatively rapid climatic oscillations are of particular interest in this framework because they provide a window into how fast biodiversity can track climatic changes in its evolutionary response (Davis and Shaw 2001; Holmes et al. 2011; Foster et al. 2013). The past 10 million years are well documented and represent one of the most climatically dynamic periods. The climate became increasingly cool following the Mid-Miocene Climatic Optimum *ca.* 15 million years ago (Ma), with a brief period of temperatures stabilizing during the Pliocene Thermal Maximum *ca.* 3.3 Ma; before the onset of Quaternary glaciations *ca.* 2.5 Ma that resulted in glacial and interglacial cycles (Haywood and Valdes 2004; Ravelo et al. 2004; Fedorov et al. 2013; Westerhold et al. 2020; Steinthorsdottir et al. 2021). These intense climatic shifts and their impact on ecological and evolutionary patterns have been the focus of an extensive corpus of studies investigating micro- to macro-evolutionary trends across a variety of model systems (e.g., Taberlet et al. 1998; Davis and Shaw 2001; Parmesan and Yohe 2003; Hewitt 2004; Schmitt 2007; Fonseca et al. 2023). Yet, some geographic areas are far less studied, and understanding fine-scale evolutionary patterns within such regions may reveal new insights into our understanding of how biodiversity can respond to climatic oscillations.

The Western Balkans are one of the main centers of endemism in the Palearctic region. The remarkable biota of this region has been shaped by a combination of rugged mountains, extensive karst systems, and complex water drainages (Griffiths et al. 2004). Apart from Albanian coastal lowlands, most of the region is covered by mid- to high-elevation mountain ranges stretching from the Accursed Mountains (Albanian Alps, Prokletije or Bjeshkët e Nemuna) in the southern Dinaric Alps, to the Pindus Mountains in the south. However, the Western Balkans are less studied than other well-known systems such as the Alps, despite intricate climatic and geological histories that make it an ideal laboratory for evolutionary studies (Krystufek et al. 2007; Schmitt 2007; Previšić et al. 2014; Ronikier and Zalewska-Gałosz 2014; Gross et al. 2021; Urzi et al. 2021; Ronikier et al. 2023). During the Miocene, major tectonic and climatic changes in the Eastern and Central Paratethys region drastically reshaped the Western Balkans (Ivanov et al. 2011; Petrušev 2021), thereby fragmenting populations and triggering geographic as well as genetic structuring across the whole peninsula. Plio-Pleistocene glacial and interglacial cycles across the region (Petrušev 2021) intensified these patterns through complex processes of geographic and genetic isolation followed in some cases by secondary contacts (Sworobowicz et al. 2015, 2020). While northern Palearctic regions were often covered by large ice sheets, the Western Balkan region had smaller, topographically restricted ice caps (Hughes 2010). These conditions allowed regional populations to survive glacial periods rather than face local extinction and, in some cases, promoted diversification (Pauls et al. 2006; Schmitt 2007; Grabowski et al. 2017; Sworobowicz et al. 2020). Although the timing of glacial expansion and retreat remains debated (López-Moreno and García-Ruiz 2025), evidence indicates that the most intense glaciation occurred around 17 ka, followed by five deglaciation phases occurring up to 13 ka (Ruszkiczay-Rüdiger et al. 2020). The lowest Equilibrium Line Altitude (ELA) for the Western Balkan ranges from 1256 m on Orjen Mountain to higher altitudes towards the south reaching 1750 m on Accursed Mountains and 1792 m on Jablanica Mountain (southwestern parts of North Macedonia; Milivojević et al. 2008; Ruszkiczay-Rüdiger et al. 2020). The limited extent of glaciation along with the complex orogeny of the region likely allowed the existence of a dense network of microrefugia that helped maintain genetic diversity over time.

Earlier investigations of evolutionary patterns and processes at different scales in the Western Balkans have laid the foundations for a better understanding of biotic assemblages through space and time (Schmitt 2007; Previšić et al. 2014; Grabowski et al. 2017). The combination of intricate orogenic cycles, emergence of diverse microclimates, and progressive dissection of water drainage systems has often restricted gene flow between populations while allowing their persistence through glacial cycles. Consequently, extant adjacent populations can show significant genetic divergences, a pattern observed across both aquatic and terrestrial systems. Despite recent progress in our understanding of regional biotic evolution, many fine-scale processes within the Western Balkans remain unclear, in particular within its rugged mountain ranges. Recent studies often focused on broader refugial structures rather than individual mountain ranges. Yet, lineages endemic to such mountainous areas are likely to show signatures of geographic isolation, genetic drift, and local adaptation. Thus, there is a need for additional fine-scale phylogeographic studies, ideally focusing on endemic and low-dispersal lineages to refine our understanding of Western Balkan biogeography.

Here we present the first genomic and biogeographic examination of the Western Balkan mountain endemic predaceous beetle, *Calosoma pentheri* Apfelbeck, 1918. This species is typically found above 2,000 m in mountain pastures with low vegetation (Fig. 1). *Calosoma pentheri* is brachypterous, with a significant reduction of its wings, resulting in flightlessness. It most frequently emerges in the spring just after snowcaps melt, but is present only for a short period before the habitat becomes too arid. However, little else is known of the species ecology, life cycle, or behavior. This Western Balkan endemic lineage was considered as two distinct species by Jeannel (1940) and by Obydov (2002); with *C. pentheri sensu stricto* distributed from Montenegro to northern Albania in Prokletija planina, Greben planina, Boris planina,

Bjelasica planina, and Čakor, and *C. relictum* Apfelbeck, 1918 distributed from eastern Albania, southwestern Kosovo and western parts of North Macedonia in mountains of Šar Planina, Korab, Deshat, Stogovo, and Bistra (Apfelbeck 1918; Jeannel 1940; Obydov 2002; Guéorguiev 2007; Bruschi 2013; Hristovski and Guéorguiev 2015; Hristovski et al. 2016). Early on, both Apfelbeck and Jeannel noted the disjunct distribution of these two and small morphological differences, most notably the surface of their elytra, with clear primary intervals forming chain-like elevations in *C. pentheri sensu stricto* that are less pronounced in *C. relictum* (Apfelbeck 1918; Jeannel 1940). In other words, the elytral sculpturing of the northern lineage is more defined than in its southern counterpart, as also noted by Obydov (2002) and Bruschi (2013). In spite of these divergences, the latter author currently recognizes a single species comprising two subspecies *C. pentheri pentheri* and *C. pentheri relictum*. Since geographical and morphological differences exist, a closer inspection of species boundaries is warranted.

The closest lineage to *C. pentheri sensu lato* is currently unknown since this species was never included in a phylogenetic framework, and morphology alone is insufficient to determine its broader systematic relationships. Despite being placed in its own genus *Microcallisthenes* Apfelbeck, 1918

Figure 1. The Western Balkan endemic *Calosoma* (*Callisthenes*) *pentheri in situ*: **A.** Habitat of *Calosoma pentheri relictum* at *ca.* 2000 m along Mount Korab slopes in northwestern North Macedonia; **B.** *Calosoma pentheri relictum* (green color morph) *in situ* in Šar Planina; **C.** *Calosoma pentheri pentheri* (coppery color morph) *in situ* in Bjeshkët e Nemuna, Maja e Rosit, Albania; **D, E.** Habitat of *Calosoma pentheri pentheri* at *ca.* 2000 m in Bjeshkët e Nemuna, Maja e Rosit, Albania. Photograph credits: Slavčo Hristovski and Emmanuel F.A. Toussaint.

upon description, the species is currently placed within the diverse Palearctic subgenus *Callisthenes* Fischer von Waldheim, 1822 (Obydov 2002; Bruschi 2013). Unfortunately, subgeneric classification within *Calosoma* Weber, 1801, largely based on Jeannel (1940), is obsolete as shown by all molecular studies to date (Osawa et al. 2004; Su et al. 2005; Toussaint and Gillett 2018; Toussaint et al. 2021; Sota et al. 2022). Even though the subgenus *Callisthenes* is one of the few clades recovered in these studies (but see Toussaint and Gillett 2018, who recovered a paraphyletic *Callisthenes*), to date only a few species have been included in phylogenetic studies and therefore the subgeneric placement of *C. pentheri sensu lato* should be considered tentative. Jeannel (1940), in his monograph, redefined the genus *Microcallisthenes* to accommodate not only this lineage (that he considered two distinct species) but also Nearctic species of *Calosoma* currently placed in the subgenus *Callistenia* Lapouge, 1929. It is therefore very likely that *C. pentheri sensu lato* belongs to the clade comprising the two subgenera *Callistenia* and *Callisthenes* that was also recovered by some molecular studies (Osawa et al. 2004; Su et al. 2005; Toussaint and Gillett 2018; Sota et al. 2022). However, the biogeographic origin of *C. pentheri sensu lato* remains unclear, despite earlier hypotheses suggesting an Anatolian origin (Casale and Vigna Taglianti 1999; Guéorguiev 2007). Given that *C. pentheri sensu lato* is brachypterous, this lineage is ideal for understanding the impact of Western Balkan paleoclimate oscillations on genomic structure and population dynamics.

In this study, we specifically test hypotheses pertaining to the evolutionary history and population dynamics of *Calosoma pentheri* across rugged mountains of the Western Balkans. We hypothesize that climatic swings in the Miocene led to periods of isolation in highland refugia that promoted strong genetic differentiation. We predict that these oscillations drove the diversification of two independent evolutionary lineages warranting recognition as two distinct species. We also predict that isolation in glacial refugia and limited connectivity among Western Balkan mountain ranges shaped pronounced population structure. To test these hypotheses, we rely on a comprehensive genomic-scale dataset combining both fresh material and natural history collection specimens.

Materials and methods

Sampling

We sampled all major known populations of *C. pentheri sensu lato* across the Western Balkans, representing the two currently recognized subspecies *C. pentheri pentheri* and *C. pentheri relictum* (Fig. 2). In total, we sampled 10 specimens of *C. pentheri pentheri* including 3 newly collected and 7 historical specimens, and 54 specimens of *C. pentheri relictum* including 37 newly collected and 17 historical specimens. Fieldwork took place in July 2003, July 2004, June 2008, June 2013 and June to July 2022 across Albania and North Macedonia. Historical specimens were sampled from the natural history collections of the Natural History Museum of Geneva (MHNG, 4 samples), Naturéum-Muséum cantonal des Sciences Naturelles (3 samples), SNSB-Zoologische Staatssammlung München (ZSM, 2 samples), Naturhistorisches Museum Basel (10 samples) and Naturhistorisches Museum Wien (8 samples).

We selected outgroups representing the closest morphological groups to the subgenus *Callisthenes* as suggested by both morphological (Jeannel 1940; Bruschi 2013) and molecular (Osawa et al. 2004; Su et al. 2005; Toussaint and Gillett 2018; Toussaint et al. 2021; Sota et al. 2020, 2022) studies. Outgroups included three museum specimens of *Calosoma* (*Callisthenes*) *marginatum* Gebler, 1830; as well as genomes of *Calosoma* (*Callistenia*) *wilkesii* LeConte, 1852 (GCA_044734065.1; Gauthier et al. 2025a), *Calosoma* (*Chrysostigma*) *tepidum* LeConte, 1852 (GCA_044734075.1; Gauthier et al. 2025a), *Calosoma* (*Castrida*) *granatense* Géhin, 1885 (GCA_022063505.1; Vangestel et al. 2024); *Carabus* (*Platycarabus*) *depressus* Bonelli, 1810 (GCA_048127345.1; Gauthier et al. 2025b); and a transcriptome of *Calosoma* (*Calosoma*) *frigidum* Kirby, 1873 (SRR13973474; McKenna et al. 2019).

Reference genome generation workflow

A specimen of *C. pentheri relictum* (DNA extraction code: CBX1095) was collected in North Macedonia from Šar Planina, in the Tetovo municipality near Vešala, on an alpine pasture near a river on the 19th of June 2022, and stored at -80 °C for genome sequencing. Tissues from the beetle thorax, head and legs were cryogenically pulverized using a Bessman Tissue Pulverizer (Thermo Fisher Scientific, Waltham, USA) and stored at −80 °C. Subsequently, high-molecular weight (HMW) DNA was extracted from the resulting powder using the MagAttract HMW DNA Kit (QIAGEN, Hilden, Germany) with proteinase K digestion. DNA quantity, purity, and fragment size were assessed by Qubit fluorescence assay and Fragment Analyzer 5200 (Agilent Technologies, Santa Clara, USA), and genomic DNA was sheared with a Megaruptor 3 (Diagenode, Liège, Belgium) to an average size of 12–15 kb (detailed in Gauthier et al. 2025a). The remaining post-extraction tissues (mostly the elytra) were mounted on a pinned archival cardboard that is deposited in the Natural History Museum of Geneva entomological dry-pinned collection with label "Toussaint lab DNA Voucher CBX1095" for future reference. The genomic library was prepared using the SMRTbell prep kit 3.0 (Pacific Biosciences, Menlo Park, USA) according to the whole genome protocol from PacBio (PN: 102-166-600). The polymerase SMRT Library complex was prepared using the Sequel® II Binding Kit 3.2 (Pacific Biosciences, Menlo Park, USA) and sequencing was performed on the Sequel IIe System (Pacific Biosciences, Menlo Park, USA) at Genesupport LifeScience (Fasteris, Plan-les-Ouates, Switzerland). Assembly was performed using Hifiasm (v0.19.8; Cheng et al. 2021) and duplications were removed using purge_dups (Guan et al. 2020). Completeness of the

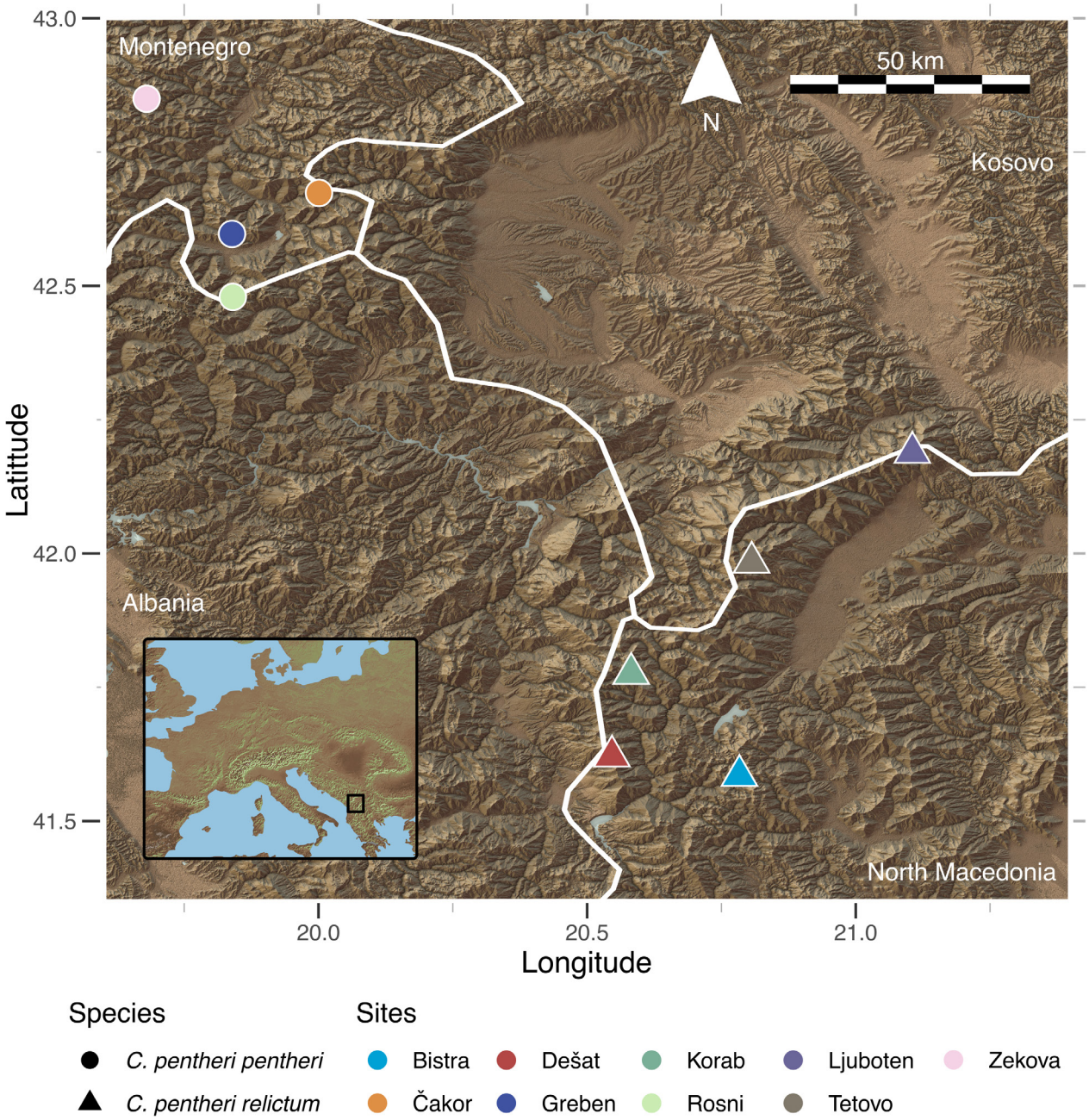

Figure 2. Sampling map of the Western Balkans. Relief map of *Calosoma pentheri* sampling localities in the Western Balkans. Sampled localities of *Calosoma pentheri pentheri* are indicated by a circle, and that of *C. pentheri relictum* by a triangle. Political borders of Albania, Kosovo, Montenegro, and North Macedonia are shown as well as an inset relief map of Europe indicating the region. The map was generated in R using rayshader (v0.40.2; Morgan-Wall 2018) and stylized in Inkscape (v1.4.2; Inkscape Project 2025).

genome was evaluated using BUSCO (Seppey et al. 2019) and the insecta_odb10 dataset composed of 1,367 genes. Genomic completeness was summarized using a snail plot generated in BlobToolkit2 (Challis et al. 2020).

hyRAD wet lab methods

Genomic DNA was obtained through destructive extraction of a single leg from each specimen using a QIAmp DNA Micro kit (QIAGEN, Hilden, Germany) and eluted in 25–50 µL of molecular grade water. A Fragment Analyzer 5200 was used to assess the quality and quantity of DNA. Seven specimens with high DNA concentrations and only limited DNA degradation were selected for probe synthesis in the hybridization capture using RAD probes (hyRAD) protocol (Suchan et al. 2016). These specimens were selected to best represent the geographic range of each lineage. hyRAD probes were prepared using a slightly modified protocol from Gauthier et al. (2023). After double-digestion with MseI and PstI-HF enzymes (New England Biolabs, Ipswich, USA), 9 µL of purified product was combined with 2.6 µL of ligation mix composed of T4 DNA ligase (New England Biolabs, Ipswich, USA) and two double-digestion RAD-sequencing adapters,

one of which contained the T7-promoter sequence required for later transcription into biotinylated RNA probes. Fifteen microliters of purified post-ligation product were PCR-amplified for 10 cycles with 15 µL of PCR mix containing Platinum™ SuperFi™ DNA Polymerase (Invitrogen, Waltham, USA) as well as double-indexed PCR primers (Integrated DNA Technologies, Coralville, USA), and divided into two PCR replicates of 15 µL each. After the two PCR replicates were combined, 3 µL of PCR mix was added to the reaction and amplified for another 10 PCR cycles. Purified post-PCR products were pooled equimolarly based on their concentration measured with Qubit dsDNA HS 1X (Invitrogen, Waltham, USA), and size-selected on a dye-free 2% agarose cassette on a PippinPrep (Sage Science, Beverly, USA) in range mode 305–405 bp. Transcription into biotinylated RNA probes was performed using HiScribe T7 High Yield RNA Synthesis Kit (New England Biolabs, Ipswich, USA).

DNA samples exhibiting a considerable amount of large fragments (> 1 kb) were processed with an extra step prior to the shotgun library preparation. CleanNGS beads (CleanNA, Waddinxveen, Netherlands) were used to purify the large DNA fragments following a double-sided size-selection protocol with a beads:sample ratio of 0.5:1 X. Those large fragments were sheared using NEBNext dsDNA Fragmentase (New England Biolabs, Ipswich, USA). The supernatant of the purification described above (containing the isolated small DNA fragments) was not discarded, but purified with CleanNGS beads with a beads:sample ratio of 1.6:1X. Both sheared large fragments and size-selected small fragments were combined and used as template for shotgun library preparation using a SRSLY NanoPlus Uracil+ NGS library preparation kit for Illumina sequencing (Claret Bioscience, Santa Cruz, USA) following the manufacturer protocol. DNA samples were divided into three categories based on their average DNA fragment size: small fragments (< 75 bp), moderate fragments (75–125 bp), and large fragments (> 125 bp). A different protocol as prescribed by the manufacturer (Claret Bioscience, Santa Cruz, USA) was used according to the fragment size during the first purification step after the phosphorylation/ligation reaction. Dual-indexing primers provided by the manufacturer (Claret Bioscience, Santa Cruz, USA) were used during the PCR step. A single-sided bead cleanup protocol was applied to purify the libraries (with a different protocol depending on the three categories described above) prior to their dsDNA quantification in a Quant-It Picogreen assay (Invitrogen, Waltham, USA). Libraries were pooled according to their concentration (with a maximum of 10 libraries per pool) and enriched by hybridization-capture following the same protocol as in Toussaint et al. (2021) with some adaptations. Only a single hybridization-capture was performed at 60 °C. A different blocking oligonucleotide was used in the hybridization mix adapted to the hyRAD probes containing an indexed P7-end. Different blocking RNA oligonucleotides solutions were prepared to block shotgun libraries with 10 bp-long i5 and i7 indexes. The pooled capture-enriched libraries were sequenced with 100 bp paired end sequencing on a NovaSeq 6000 (Illumina, San Diego, USA) and demultiplexed at the iGE3 Genomics Platform of the University of Geneva (https://ige3.genomics.unige.ch).

In silico reference-catalog design

We did not sequence capture probes, as often done in the framework of standard HyRAD and PHyRAD bioinformatic pipelines (Schmid et al. 2017; Toussaint et al. 2021). Therefore, we modified the PHyRAD pipeline by using the newly generated reference genome to map the captured library sequences. We selected six samples that best represented the biogeographic distribution of the two *C. pentheri* lineages to build an *in silico* reference catalog. These samples were processed and had quality control performed as described in the section HyRAD bioinformatic workflow, and then mapped against the *C. pentheri relictum* genome using BWA-MEM (v0.7.17; Li and Durbin 2009). We kept mapped regions with at least 100x coverage and 100–300 bp in length to identify putative regions of the *in silico* reference catalog using bedtools (v2.3; Quinlan 2010) genomecov and merge for each of the six samples. The selected mapped reads were combined in two steps using bedtools merge, first by identifying mappings unique to each lineage (e.g., *C. pentheri pentheri* and *C. pentheri relictum* specific mappings) and then merging again to identify those found in both lineages. Once combined, mappings greater than 300 bp were excluded using bedtools cluster followed by bedtools getfasta to extract the reference catalog from the reference genome and generate the *in silico* reference catalog.

HyRAD bioinformatic workflow

We performed quality control and preprocessing of raw reads using fastp (v0.23.4; Chen et al. 2018) for adapter trimming and read quality filtering using default options. Before processing in our pipeline, publicly available long-read genomes (GCA_044734065.1; GCA_044734075.1; GCA_048127345.1) and our new *Calosoma pentheri relictum* genome were processed into 100 bp "pseudo-short reads" using a custom python script (simulate_reads.py). This enabled consensus reads and variant calling to be generated in downstream workflows. All custom scripts are available at https://github.com/crcardenas/Balkans_calosoma.

We slightly modified the phyloHyRAD pipeline (Gauthier et al. 2020) by excluding the PCR duplicate step, otherwise the bioinformatic pipeline was identical to the established workflow. The "pseudo-short" and paired-end reads were mapped against the *in silico* reference catalog, duplicate reads were cleaned, and indels were realigned using the picard suite (v2.27.4; Broad Institute 2019) and samtools (v1.4; Li et al. 2009). Because data from museum specimens was included, we further processed the mapped reads using mapdamage2 (v2.0; Jónsson et al. 2013) to account for the potential presence of cytosine deamination, a typical post-mortem DNA damage.

All mapped and processed reads were used for variant calling and orthologous locus generation. To generate independent variants we used GATK HaplotypeCaller (v4.5; Poplin et al. 2017), and created a filtered dataset called **all_snps** using VCFTools (v0.1.17; Danecek et al. 2011). We also used VCFtools to generate SNP statistics for each sample. We generated two subsets of the **all_snps** dataset using the same VCFTools flitering parameters for downstream population genetic analyses; one named **penrel** with only *C. pentheri relictum* specimens and another **subspp** with specimens of both *C. pentheri* lineages. Preliminary filtering showed that four samples (CBX0664, CBX0683, CBX0898, and CBX0905) contained > 90% missing SNPs, and these were subsequently removed from the population genetic analyses. For downstream SNP phylogenetic inferences, we created another subset of the **all_snps** dataset called **basic_snps** using the same flags in VCFtools except that the max-missing flag was lowered to 75%.

For locus-based phylogenetic datasets, we slightly modified the phyloHyRAD pipeline for locus discovery using a minimum read coverage of 3 and minimum consensus length of 100 bp using a custom script (consensus_loci.sh). Of the loci meeting these criteria, we retained only non-duplicate sequences from the "*in silico* reference catalog".

Population genomic analyses

To confirm ambiguous localities and summarize the haplotypes recovered, we performed a principal components analysis (PCA) using R (v4.5.1; R Core Team 2025); for both **penrel** and **subspp** datasets. These datasets were imported using vcfR (v1.15; Knaus and Grünwald 2016, 2017) and allele counts with missing data were replaced by the mean allele frequency using adegenet (v2.1.11; Jombart 2008; Jombart and Ahmed 2011). The PCA was visualized using ggplot2 (v4.0; Wickham 2016).

We further estimated genetic clustering using STRUCTURE (v2.3.4; Pritchard et al. 2000). Both the **penrel** and **subspp** datasets were converted into a STRUCTURE compatible file (Clark 2017) without locality assignments. For each dataset, we performed two independent analyses with and without admixture, 100,000 steps and a 50,000 burn-in, along with five replicates for each independent analysis. We tested for clusters (K) of one through eight and one through ten for the **penrel** and **subspp** datasets respectively. We assessed the analyses using pophelper (v 2.3.1; Francis 2017) in R to identify the best K value, address label switching, and visualize structure plots.

We estimated Hardy-Weinberg Equilibrium (HWE) using pegas (v1.3; Paradis 2010) and genetic diversity with hierfstat (v0.5-11; Goudet 2005) for both datasets. Importantly, studies have shown that population genetic statistics can be estimated accurately with relatively few taxa (e.g., 2–3) and thousands of sites (Nazareno et al. 2017). Therefore, we included localities sampled with only 2–3 individuals in these analyses. We estimated isolation by distance by comparing the pairwise fixation indices and geographic distances to examine evidence of isolation by distance. Geographic distances for each locality were identified by estimating the Mercator coordinates of all samples from a site using geosphere (v1.5-20; Hijmans 2019).

Supermatrix phylogenetic inferences

To infer phylogenetic relationships across *C. pentheri sensu lato*, loci were aligned using MAFFT (7.505; Katoh and Standley 2013) and locus summary statistics were estimated using AMAS summary by taxon (Borowiec 2016) and a custom python script (summary.py). Loci with less than 90% locus occupancy were removed from the dataset. We excluded loci with >50% ambiguous sites, i.e, loci containing excessive gaps ("-") or unknown nucleotides ("N"). The remaining loci were trimmed using trimal -automated1 (v1.4; Capella-Gutiérrez et al. 2009). A final supermatrix called **ml_filt**, with 90% locus occupancy (N = 70 taxa) was generated using AMAS concat.

The optimal partitioning scheme for the final supermatrix was identified with ModelFinder as implemented in IQ-TREE (v2.3.6; Kalyaanamoorthy et al. 2017; Minh et al. 2020), and selected using the Bayesian Information Criterion (Chernomor et al. 2016). Maximum likelihood (ML) phylogenetic inference was performed using IQ-TREE with 1,000 ultrafast bootstrap replicates (UFBoot; Hoang et al. 2018), with the -bnni flag, and 1,000 SH-like approximate likelihood ratio tests (SH-aLRT; Guindon et al. 2010). The ML inferences were performed by analyzing all nearest-neighbor interchanges with the -allnni flag, and conducting 20 independent tree searches. Combined values of SH-aLRT ≥ 80 and UFBoot ≥ 95 were considered robust for a given branch. We also calculated locus and site concordance factors in IQ-TREE. To do so, we generated individual locus trees using IQ-TREE and models of nucleotide substitution for each locus estimated using ModelFinder. Lastly, we created a final supermatrix called **ml_nohist**, with only modern specimens to avoid potential biases linked to historical specimens (22 samples removed, **ml_nohist** N = 48), and analyzed this dataset using identical parameters in IQ-TREE as described previously.

SNP phylogenetic inferences

We performed phylogenetic inferences using the **all_snps** dataset from the population genetic analyses. We first created four subsets 1) **basic_snps** as described previously in the variant calling step 2) **no_hist**: removal of all samples with >20 years between the date of sampling and DNA extraction, 3) **no_Ts**: to examine the effect of potential deamination we removed all transitions using a custom script (remove_VCF_Ts.awk), and 4) **no_Ts_no_hist**: removal of transitions and all historical specimens. For each of the four SNP datasets, we used Vcf2phylip (v2.0; Ortiz 2019) and raxml_ascbias.py (https://github.com/btmartin721/raxml_ascbias) to create a final matrix with invariant sites

removed. Phylogenetic analyses were performed in IQ-TREE using the ascertainment bias correction model and 20 independent runs with 1,000 UFBoot replicates.

Coalescent-based species tree inferences

We performed species tree inferences using the locus trees from the **ml_filt** dataset in a coalescent framework using wASTRAL (v1.22.3.7; Zhang and Mirarab 2022) to account for missing data and locus tree uncertainty. We ran wASTRAL using increased sampling and subsampling and calculated bootstrap branch support.

Divergence time estimation

We generated a dataset called **divergence_loci** to infer divergence estimates, selecting a single specimen per locality with the fewest undetermined/ambiguous characters as well as the most recovered loci per sampling site (including outgroups N = 15). For the generation of the **divergence_loci** matrix, we selected loci with a minimum length of 100 bp and 9 taxa per locus; phylogenetic inference was performed in the same manner as in the previous Phylogenetic methods section.

We used a gene-shopping approach with SortaDate (Smith et al. 2018) and phyx (Brown et al. 2017) to identify 300 clock-like loci that have the least topological conflict and similar length to the **divergence_loci** ML tree. For the SortaDate analysis, loci containing the *Carabus* outgroup were identified using a custom python script (sortadate_helper.py; available from https://github.com/crcardenas/Sortadate_IQTree2_helper). Once optimal loci were selected we used PartitionFinder2 (v2.1.1; Lanfear et al. 2016) with a minimum subset size of 2000 bp to identify the optimal partitioning scheme of the new matrix and to limit overparameterization. The most likely substitution models available in BEAST (v1.10.4; Suchard et al. 2018) were identified for each resulting partition using ModelFinder as implemented in IQ-TREE. The selected 300 loci were combined in a dataset called **divergence_model** and subjected to the same phylogenetic methods as described previously. The phylogenies inferred with the **divergence_model** and **divergence_loci** datasets were compared for topological congruence. Finally, the **divergence_loci** phylogeny was made ultrametric using the R package phytools function chronotree (v2.5.5; Revell 2024) based on the median age estimates of Cardenas et al. (2025).

To perform divergence time estimation in BEAST, each of the partitions identified for the **divergence_model** was assigned an uncorrelated lognormal relaxed (UCLR) molecular clock and the nucleotide substitution models identified in ModelFinder. The mean rate under the UCLR molecular clock for each partition was set up with a uniform prior distribution, a starting value of 0.01, and a range of 1.0e-08–1.0. The following two secondary calibrations derived from Cardenas et al. (2025) were used: *Carabus* + *Calosoma* (Median 44.09 [40.53–47.78] Mya) and the crown of *Calosoma* (Median 22.58 [20.81–24.95] Mya). Each calibration was set up with a lognormal prior distribution for the corresponding node age parameter with 95% of the distribution fitting the 95% highest probability density (HPD) interval estimated in Cardenas et al. (2025). The following priors were used in BEAUti to set up these parameters: (*Calosoma* + *Carabus*) mean = 40.073 standard deviation = 1.849, and offset = 3.96; crown of *Calosoma* mean = 19.21, standard deviation = 1.058, and offset = 3.589. We performed two separate analyses using different tree priors, the coalescent constant population size and the speciation Yule pure birth models. For each of the separate tree priors, we conducted 100 million steps with five independent runs sampling parameters every 1000 steps for both models on the University of Geneva, Switzerland, Bamboo HPC service. We examined the operator files of all analyses to ensure a reasonable acceptance ratio. The log files of each replicate were examined in Tracer (v1.7.2; Rambaut et al. 2018) and were considered acceptable if moderate to good convergence was achieved (ESS ≥ 100 and ESS ≥ 200 respectively). For each model, the best performing replicate was selected based on Tracer values, effective sampling size, and likelihood. A maximum credibility clade tree was generated in TreeAnnotator (v1.10.4; Suchard et al. 2018) with a 10% burn-in fraction. The resulting chronogram is hereafter referred to as **BEAST_tree**.

Estimates of admixture

The program Dsuite (v0.5; Malinsky et al. 2021) was used to estimate the degree of admixture between sampled localities and species using the BEAST chronogram. The F-ratio statistic was used rather than Patterson's D statistic given the small size of genomic loci used in this study. This statistic can be applied to F-branch statistics (F_b) in Dsuite, so that evidence of gene flow can be inferred from a tree. Significance tests using a z-score ≥ 3 for the F4-ratio test were used as evidence of introgression between branches of the phylogeny. Finally, F-branch scores were used to describe the degrees of significant admixture. An additional subset of variants were generated using the aforementioned phylohyRAD methods, including only the one *C. marginatum* and the select *C. pentheri sensu lato* samples used in the divergence estimates. Finally, the **BEAST_tree** chronogram was pruned using phytools to keep only these samples for analysis.

Results

Reference genome generation workflow

Extraction of HMW DNA from the *Calosoma pentheri relictum* specimen resulted in 1935.5 ng of genomic DNA available for sequencing (19.6 ng/μL, 100 μL elution volume). PacBio HiFi sequencing returned 482,541 reads (4.38 Gb) with an average size of 9.1 kb and an N50 of 10.4 kb. During processing, 7.7 Mb of duplicates were

removed. The final assembly contained 595 scaffolds, an N50 of 2.4 Mb, a total length of 214.8 Mb, and 98.6% genome completeness based on the universal single-copy ortholog gene set for Insecta (BUSCO; Fig. 3). Given the size of the final assembly, sequencing depth was *ca.* 19x.

In silico reference catalog

A total of 88,540,086 reads (median 15,217,899; SD 2,104,681) from samples used in the *in silico* reference catalog design mapped to the reference genome. Per lineage mapping statistics: *C. pentheri pentheri*: 41,882,382 (median 13,648,641; SD 1,585,464) and *C. pentheri relictum*: 46,657,704 (median 16,354,771; SD 3,080,393). Once merged, a total of 45,355 (median 7,110; SD 1,777) unique mappings were identified. Unique mappings per lineage: *C. pentheri pentheri*: 22,084 (median 7,468; SD 1,278) and *C. pentheri relictum*: 23,271 (median 6,752; SD 2,480). After filtering for overlapping loci, a total of 18,716 unique targeted loci were retained in the final *in silico* reference catalog.

Sequencing results and hyRAD data recovery

Post quality control, 361,781,487 short reads were recovered (median 4,905,647; SD 3,063,892). mapDamage did not detect significant post-mortem damage in the data

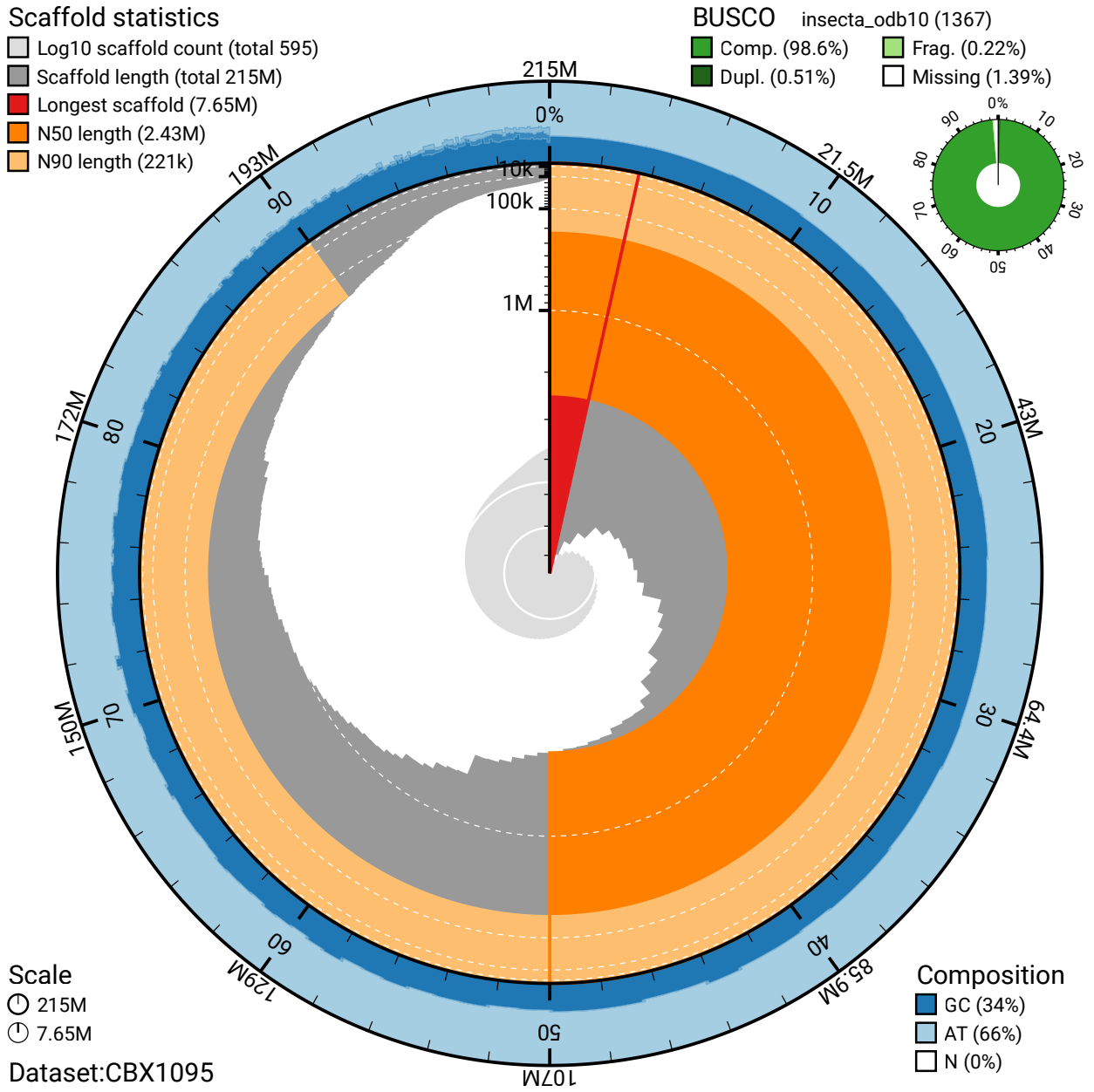

Figure 3. Snail plot of the newly generated *Calosoma* (*Callisthenes*) *pentheri relictum* genome. The descriptive statistics described are the total length, the N50 and N90 lengths, the longest scaffold identified, GC and AT composition. Results of BUSCO recovery using the insecta_odb10 database are shown along with statistics regarding completeness, duplicates, fragmentation, and missing genes in the final assembly.

(see supplemental data). Processed long-read outgroup samples mapped a total of 23,300,120 pseudo-short reads (median 4,316,496; SD 3,763,656) to the reference catalog. For all samples we recovered 619,473,276 (median 7,537,381; SD 5,183,844) reads that mapped to the "*in silico* reference catalog".

A total of 344,568 variant sites were identified. Filtering resulted in 11,799 sites with a median of 2,679 (SD 3,026) missing sites for the **penrel** dataset, and 11,928 sites with a median of 2,525 (SD 2,328) missing sites for the **subspp** dataset. A median of 18,637 loci was recovered per sample (SD 3,485.756) with a median contig length of 191 bp (SD 3) per sample. Per sample statistics are available in Suppl. material 1.

Population genetic analyses

The PCA revealed genetic differentiation between *C. pentheri pentheri* and *C. pentheri relictum* as well as between distinct populations of *C. pentheri relictum*. Analysis of the **penrel** dataset using 4,168 SNPs explained 32.3% of the variation with the first two principal components (Fig. 4A) explaining the most variation in the data. There was a marked decrease in variance explained as additional components were explored (Fig. 4A, B). Both PCA visualizations of the **penrel** data (Fig. 4) indicated that Bistra and Tetovo are distinct from the rest of the *C. pentheri relictum* localities. Samples from Dešat, Korab and Ljuboten displayed less variation but with otherwise good clustering by locality.

Using PCA results, we inferred the most likely localities of museum specimens with ambiguous or missing collection events. The placement of CBX0362 through CBX0364 in Korab was within the 95% confidence intervals for all three PCA axes presented. The labels of samples CBX0607 and CBX0608 had no information on locality but we found them clustering with the rest of the Bistra samples.

The principal components analysis of the **subspp** dataset (5,286 SNPs which explained 52.5% of the variation), revealed clear separation between the two subspecies (Fig. 5). The inferred localities of the *C. pentheri relictum* samples were used for presentation. The first two principal components explained the most variation (Fig. 5A), while PC2 and PC3 (Fig. 5A, B) explained the most variation within *C. pentheri relictum*.

STRUCTURE analyses revealed discrete clusters of the *C. pentheri* lineages and evidence of admixture within *C. pentheri relictum*. For the **subspp** dataset, the optimal number of clusters was estimated as K = 2 (ΔK = 3806.433; Table 1, Suppl. material 2: fig. S1). The admixture STRUCTURE plot consistently recovered discrete populations for both subspecies across all K values examined (Fig. 6; see also Suppl. material 2: fig. S1 for all K estimates). Values of K = 5 and K = 4 evidenced admixture, while greater K values (5–10) reflected minor

Table 1. Table of K estimates of the **subspp** dataset using the Evanno deltaK method. The table shows the deltaK estimates for the **subspp** STRUCTURE analysis of *C. pentheri* lineages (N = 56) that includes admixture. The columns are: k = Value of K; elpdmean = Mean estimated ln probability of data, elpdsd = mean estimated ln probability standard deviation, and deltaK = Evanno deltaK estimate. The best K estimates based on the data are shown in bold. Estimates were generated using pophelper in R. Full pophelper output can be found in Suppl. material 1.

k	elpdmean	elpdsd	deltaK
1	-69961.16	2.303	NA
2	**-53361.58**	**4.029**	**3806.433**
3	-52097.72	1321.028	0.12
4	-50674.88	767.604	3.598
5	-52013.54	1711.67	8.76
6	-68347	38087.971	0.348
7	-97943.5	86339.396	0.079
8	-120702.4	153690.292	0.593
9	-52386.64	2044.129	54.494
10	-95464.16	86849.881	NA

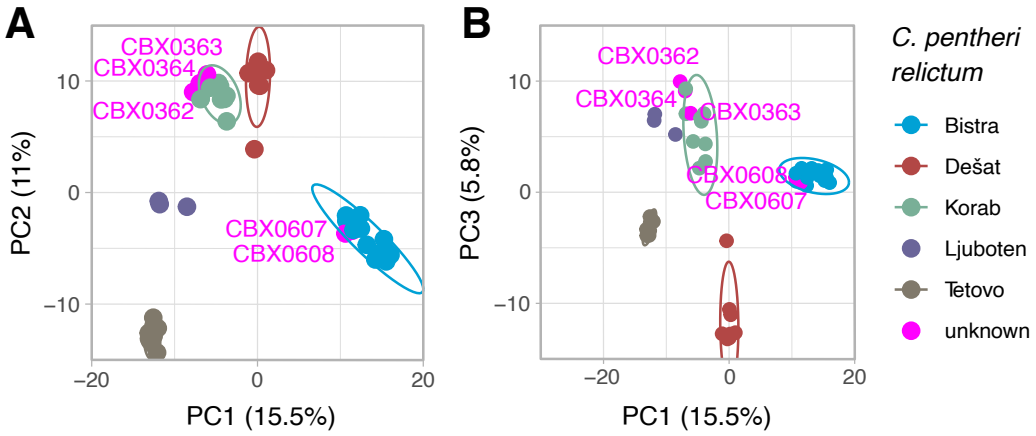

Figure 4. Principal components analysis of the **penrel** dataset. **Panel A** shows the principal components 1 and 2 with 26.5% of the variation found within the *C. pentheri relictum* samples (N = 48). **Panel B** shows the principal components 1 and 3, with 21.3% of the variation found. Only three samples came from Ljuboten, and therefore no confidence interval (ellipses) could be estimated. Samples with historical specimen locality uncertainties coded as magenta and labels were retained in the figure, and their confidence interval excluded. Figure stylized in Inkscape.

variation within existing clusters rather than revealing new ones. STRUCTURE analyses of the **subspp** dataset under the no-admixture model recovered the same discrete clusters but showed no evidence of admixture or intra-cluster variation (Suppl. material 2: table S1, fig. S2).

Clustering patterns in the **penrel** dataset were largely consistent with the **subspp** dataset. The best-supported K was also 2 (ΔK = 94.536; Suppl. material 2: table S2; see also Suppl. material 2: fig. S3), separating the populations into Ljuboten+Tetovo and Bistra clusters (Fig. 6). Evidence of admixture between these clusters was observed in the Korab and Dešat localities. An additional third cluster was recovered at a K = 3 (ΔK = 60.634; Suppl. material 2: table S2), whereas greater K values increased intra-cluster variation without identifying additional discrete clusters (Suppl. material 2: fig. S3). The no-admixture analyses recovered the same discrete clusters as observed in the **subspp** dataset (see Suppl. material 2: table S3, fig. S4). Samples with ambiguous or missing collection data consistently clustered with their respective localities, corroborating PCA analyses.

Population genetic analyses indicated clear differentiation between the two *C. pentheri* lineages. Comparison of

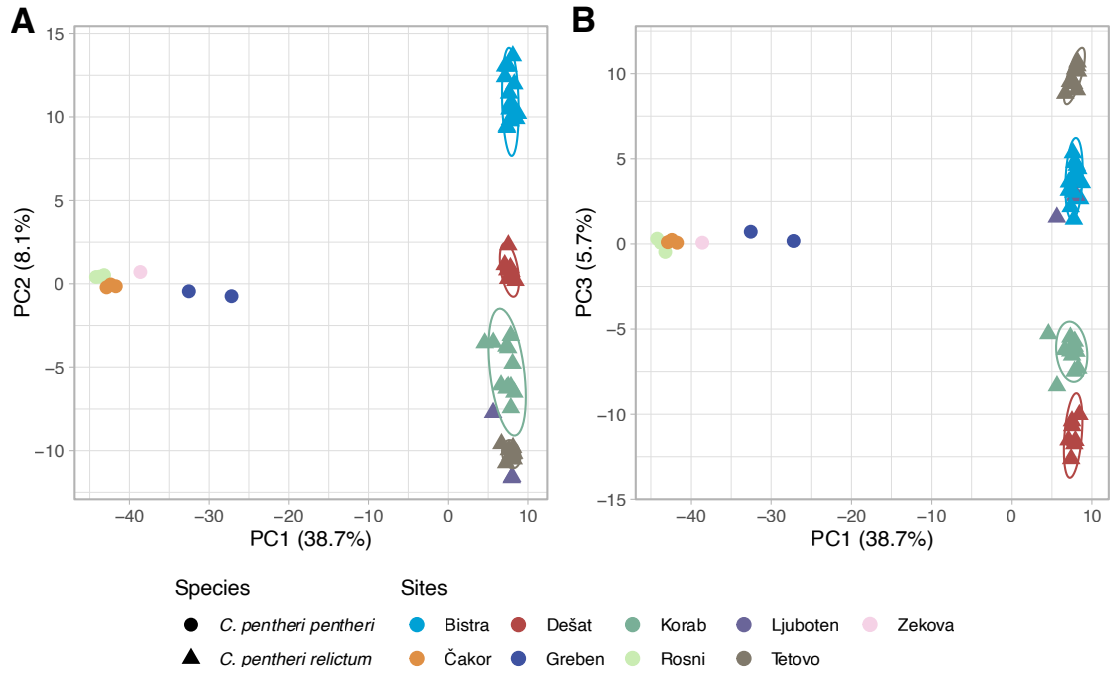

Figure 5. Principal components analysis of the **subspp** dataset. Panel A shows the principal components 1 and 2 with 46.8% of the variation found in both *C. pentheri* lineages (N = 56). Panel B shows the principal components 1 and 3, with 44.4% of the variation found. All *C. pentheri pentheri* localities and the *C. pentheri relictum* samples from Ljuboten do not have confidence intervals (ellipses) because each included three or fewer samples. Figure stylized in Inkscape.

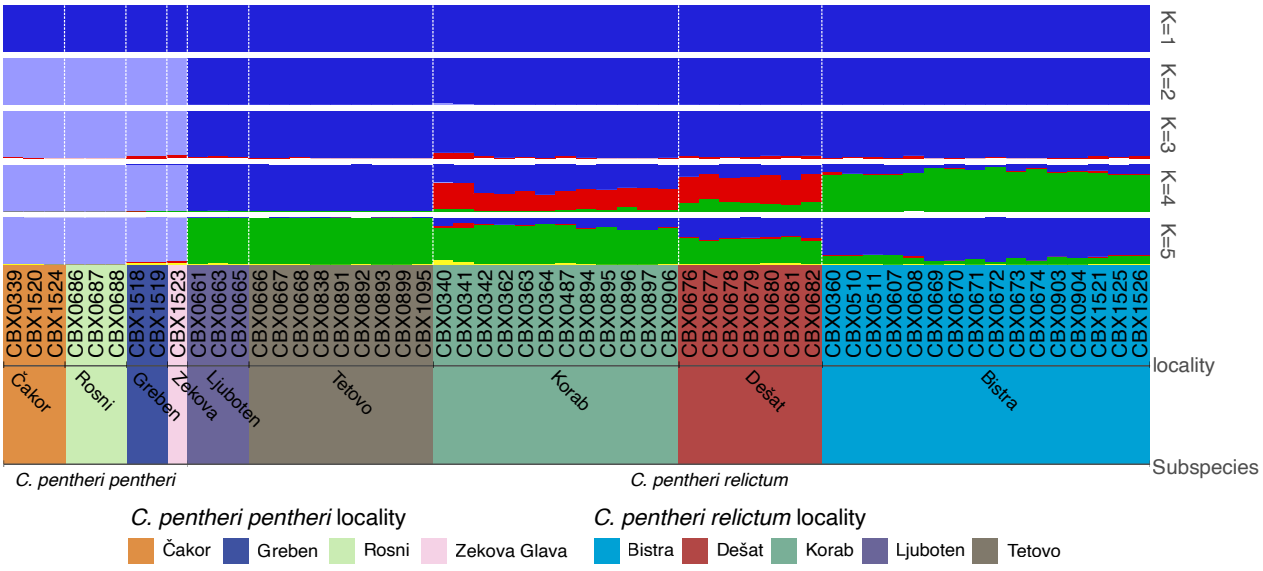

Figure 6. STRUCTURE analysis of the **subspp** dataset. Results of the STRUCTURE analysis of *C. pentheri* lineages (N = 56) with admixture plots showing population cluster estimates of K 1–5 in the **subspp** dataset. The STRUCTURE plot was generated using pophelper in R, samples are ordered from north to south, and stylized in Inkscape.

both lineages (**subspp** dataset) with the *C. pentheri relictum* lineage alone (**penrel** dataset), revealed higher observed heterozygosity (H_o) than expected (H_s), low levels of gene diversity (total gene diversity H_t, corrected gene diversity H_t', and corrected gene diversity among samples D_{st}'), and low levels of inbreeding (F_{is}; Table 2). Fewer sites conformed to the HWE when both lineages were analyzed together than when only *C. pentheri relictum* was considered. Furthermore, gene diversity estimates were higher when both lineages were analyzed together, while both datasets maintained low levels of inbreeding. Comparison of the **subspp** and **penrel** datasets indicated low inbreeding in both, although slightly higher levels were observed in comparison with the *C. pentheri relictum* data. Finally, fixation indices indicated strong differentiation between the two lineages (F_{st}' = 0.474) and moderate population structure within *C. pentheri relictum* (F_{st}' = 0.176).

Comparison of pairwise fixation indices across geographic distances provided clear evidence of isolation by distance between the two lineages (Fig. 7A). Further comparison of fixation indices between *C. pentheri pentheri* and *C. pentheri relictum* localities revealed evidence of strong genetic differentiation at larger geographic distances. In contrast, comparisons within each lineage (e.g., *C. pentheri relictum* to other *C. pentheri relictum* localities) showed lower levels of genetic differentiation. In the *C. pentheri pentheri* localities (Fig. 7B) fixation indices did not show an increase with geographic distance. The *C. pentheri relictum* localities (Fig. 7C) exhibited a positive linear relationship, with fixation indices increasing as geographic distances grow.

Phylogenetic results

Supermatrix phylogenetic inferences

Substantial locus recovery was achieved in both the **ml_filt** and **ml_nohist** datasets, with minimal missing data. Following taxon filtering, selection of loci with ≥90% locus occupancy, alignment, and trimming, an average of 2,815 loci per sample (SD 536) was recovered, with an average locus length of 179 bp (SD 4) per sample. Both matrices used for ML inferences comprised 2,231 loci (Table 3). Inclusion of historical samples slightly increased the fraction of parsimony-informative sites (Table 3), whereas removal of these samples led to a corresponding increase in invariant sites.

Across all supermatrix phylogenetic analyses, both *C. pentheri* lineages were recovered as monophyletic, with strong branch support (Fig. 8, and Suppl. material 2: figs S5, S6). Apart from the two localities, Čakor and Korab in both lineages, all other localities were consistently monophyletic and well supported. Regardless of whether historical samples were included, Bistra was recovered as sister to the remaining *C. pentheri relictum* localities.

Concordance factors for deep splits in both **ml_filt** and **ml_nohist** datasets indicated that only a few genes and sites were decisive (Suppl. material 2: figs S7–S10). Within the **ml_filt** dataset, the *C. pentheri relictum* populations exhibited the lowest gene and site concordance factor scores (gCF and sCF), with many loci being indecisive. Notably, the split between Bistra and the remaining *C. pentheri relictum* populations was supported by a higher percentage of loci and sites (9.64% and 66.3% **ml_filt**; and 11.7% and 56% **ml_nohist**) compared to most other *C. pentheri relictum* populations. Removing historical samples marginally increased the number of concordant loci (Suppl. material 2: figs S9, S10). Site concordance factors generally showed higher values, but only a minority of loci and SNPs supported the recovered relationships.

SNP phylogenetic inference

When filtering by historical samples or transitions (Ts), both approaches reduced the total number of variant sites in the SNP datasets, but removal of historical samples showed that these datasets contained more invariant sites and, conversely, fewer parsimony-informative sites (Table 4). A marginal increase in the number of singleton sites was observed in datasets with Ts removed. The phylogenetic analyses of

Table 2. Global population genetic statistics. Global estimates of both **subspp** and **penrel** datasets population genetic statistics: number of taxa (n), number of sites (e.g., SNPs), Hardy-Weinberg equilibrium (HWE), observed heterozygosity (H_o), expected heterozygosity (H_s), total gene diversity (H_t), inbreeding coefficient (F_{is}), corrected gene diversity (H_t'), corrected gene diversity among samples (D_{st}'), fixation index (F_{st}), and population corrected fixation index (F_{st}').

dataset	n	sites	HWE	H_o	H_s	H_t	F_{is}	H_t'	D_{st}'	F_{st}	F_{st}'
subspp	56	4168	82.12%	0.077	0.057	0.104	-0.335	0.110	0.055	0.445	0.474
penrel	48	5286	90.02%	0.081	0.063	0.074	-0.288	0.014	0.010	0.146	0.176

Table 3. Statistics for datasets used in supermatrix phylogenetic analyses. Columns contain the following information: datasets with their respective taxon count, percentage of missing data % (missing), mean contig length after trimming, alignment length (bp) (length), distinct number of patterns in the alignment (distinct), PIS = parsimony-informative sites (PIS), and invariant sites (IS).

Dataset (N)	loci	missing %	length (bp)	distinct	PIS	IS
ml_filt (70)	2,231	7.17	426,321	78,009	19,446	380,387
ml_nohist (48)	2,231	8.63	426,321	46,130	17,259	384,708
divergence_loci (15)	1,798	12.15	355,040	11,605	12,289	317,621
divergence_model (15)	300	8.60	62,291	4,494	3,696	52,331

all SNP datasets recovered the same backbone topology as the ML tree, except for the placement of *C. frigidum*. In all SNP analyses, the *C. pentheri* lineages were consistently recovered as reciprocally monophyletic with strong branch support. Localities of *C. pentheri* always formed well-supported clades, but topological relationships among those clades were inconsistent when all transitions were removed. The SNP analysis of *C. pentheri relictum*, excluding the **no_Ts_no_Hist** dataset, recovered Bistra(Dešat(Korab(Korab-Hist(Ljuboten+Tetovo)))) (see Fig. 8, and Suppl. material 2: figs S11–S13). When historical samples were included, we recovered the Korab locality as paraphyletic in agreement with the ML tree (Suppl. material 2: figs S11, S13).

Coalescent-based species tree inferences

The wASTRAL coalescent-based analysis recovered some relationships that contradicted the ML and SNP phylogenetic results (Suppl. material 2: figs S14, S15). Among outgroups, the relationship between *C. frigidum* and *C. granatense* was inconsistent with the ML tree. Additionally, *C. marginatum* was recovered as sister to *C. pentheri pentheri* rather than to both *C. pentheri* lineages. Within both *C. pentheri* lineages, one sample was recovered as sister to the remaining samples, rendering one locality paraphyletic (*C. pentheri pentheri*: CBX0338 Čakor and *C. pentheri relictum*: CBX0905 Bistra, and CBX684, CBX683 Dešat). Apart from these relationships, the *C. pentheri relictum* localities followed a pattern similar to that observed in the **ml_filt** dataset.

Divergence time estimation

When selecting samples for the **divergence_loci** dataset, the *C. pentheri relictum* genome did not recover the largest number of loci, likely due to variation introduced during processing of long reads into pseudo-reads. However, CBX0892 from Tetovo rather than the new genome, likely because it was used in the design of the "reference catalog". Thus, we

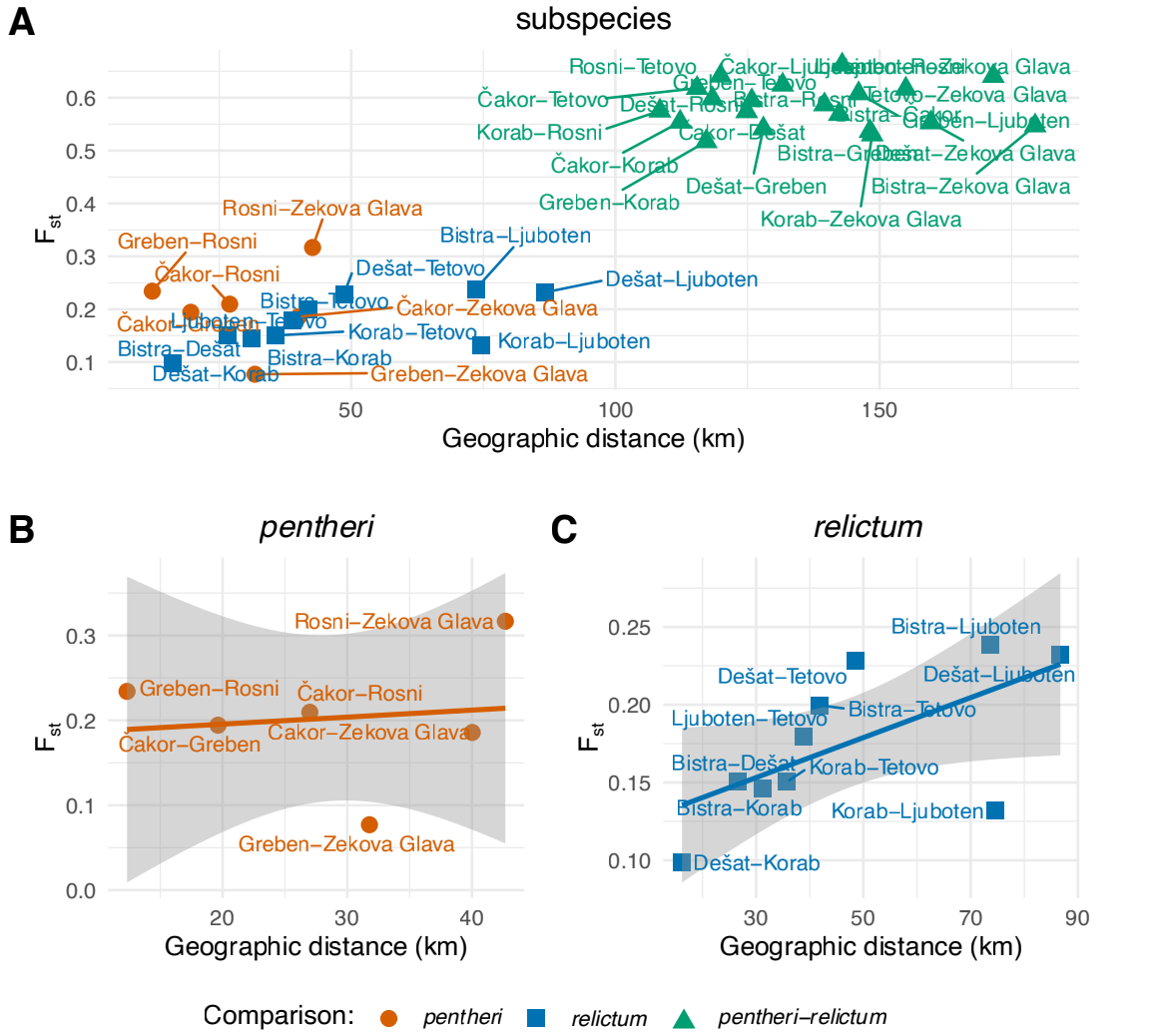

Figure 7. Pairwise comparison of F_{st} by geographic distance within and between both lineages. Pairwise comparisons of F_{st} by geographic distance for (**A**) both *Calosoma pentheri* lineages (N = 56), (**B**) *C. pentheri pentheri* (N = 8), and (**C**) *C. pentheri relictum* (N = 48). Within each plot, the y-axis represents the estimated F_{st} values, and the x-axis represents the geographic distances (measured in kilometers). Individual pairwise comparisons of localities are indicated in the plots with text labels: *C. pentheri pentheri* represented by an orange circle, *C. pentheri relictum* by a blue square, and both lineages by a green triangle.

Table 4. SNP dataset statistics used in phylogenetic inference. Statistics for the SNP datasets used in ML phylogenetic inference. Column information: dataset and number of taxa in the dataset, number of of SNPs in the dataset (sites), count of transitions and transversions (Ts/Tv), number of invariant sites removed before phylogenetic analysis (IS removed), length of the matrix (length), parsimony-informative sites (PIS), singleton sites, best run in ML independent tree searches (best run), and log-likelihood of the best run.

dataset (N taxa)	sites	Ts/Tv	IS removed	Length	PIS	singleton sites	best run	log- likelihood
basic_snps (70)	10794	6427	1771	9023	6071	2952	19	-174907.380
no_hist (48)	10734	6417	3066	7668	4842	2826	14	-117566.342
no_Ts (70)	10543	0	1714	8829	5773	3056	8	-156189.674
no_Ts_no_hist (48)	10453	0	2764	7689	4693	2996	11	-106641.795

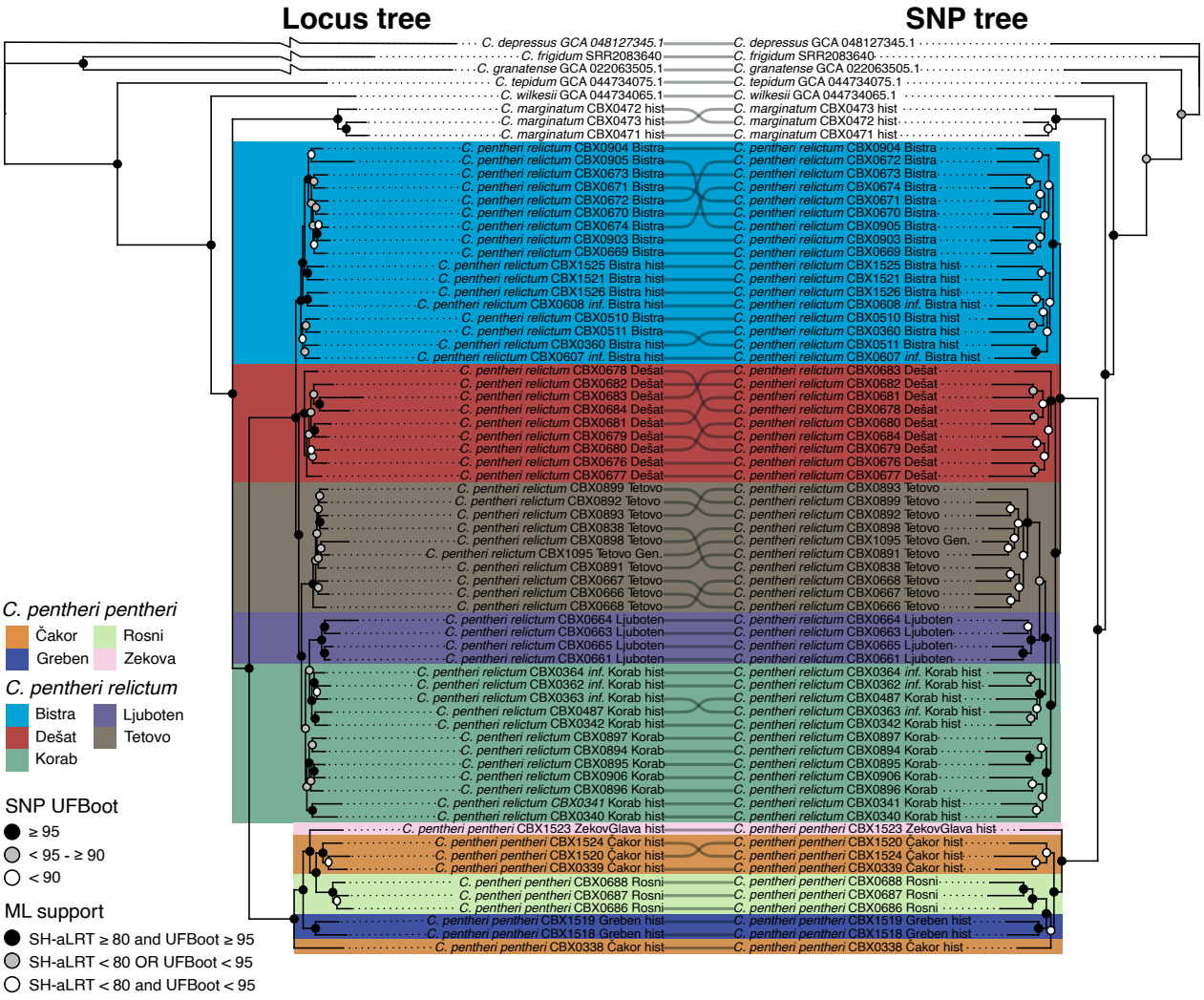

Figure 8. Cophylogeny plot of the maximum-likelihood supermatrix and SNP phylogenetic inferences. Maximum likelihood (ML) phylogenetic trees, based on supermatrix (**ml_filt**, N = 70) and SNPs (**basic_snps**, N = 70) presented as a co-phylogeny, with sample tip labels connected by lines between the two trees. Taxa with inferred localities, based on PCA and STRUCTURE analyses are indicated by "CBX# *inf.* Locality" in the tip labels. Outgroup branches were shortened to make the *C. pentheri* clades more visible in the ML trees. Stylization and aesthetic adjustments were made in Inkscape.

identified 1,213 loci that included the *Carabus* outgroup in the **divergence_loci** dataset. Following gene shopping and partitioning, eight partitions were recovered in the **divergence_model** dataset (see Table 3, and Suppl. material 2: table S4). The inferred topology of the **divergence_loci** and **divergence_model** trees (Suppl. material 2: figs S16, S17) closely matched other ML estimates. The only deviation involved the placement of *C. frigidum* among the outgroups, where it was recovered as sister to *C. granatense* (Suppl. material 2: fig. S18). Finally, the placement of the *C. pentheri relictum* Korab population was consistent with other ML phylogenetic inferences excluding historical samples.

All five replicates of the different tree model analyses, using the fixed topology from the divergence_loci tree, recovered consistent divergence time estimates in BEAST. Across all BEAST analyses, partition one and seven exhibited

slightly low operator acceptance ratios (~ 0.18–0.19), and the node height acceptance ratios were low (~ 0.08). Otherwise, review of the log files in Tracer revealed that most parameters had acceptable ESS values and stable traces. The only exception was the ESS of ucl.mean and ucld.stdev in partition four (replicate four ucld.mean ESS = 155, and ucld.stdv ESS = 182). All replicates had median likelihood values ranging from -161,332.9770 to -161,332.7218. Replicate one of the coalescent constant model was selected to present the divergence analysis (Fig. 9) We estimated median ages for the root (*Calosoma* + *Carabus*) at 41.05 Ma [38.04–44.24] 95% HPD interval, crown *Calosoma* at = 23.86 Ma [21.8879–25.8943], crown *Callisthenes* at 7.64 Ma [6.6.48–8.89], crown *Calosoma pentheri sensu lato* at 6.14 Ma [5.15–7.18], crown *Calosoma pentheri pentheri* at 2.58 Ma [2.11–3.12], and crown *Calosoma pentheri relictum* at 1.69 Ma [1.37–2.03] (Suppl. material 2: fig. S18).

Evidence of admixture

Analysis of SNP data using the f4-ratio test provided evidence of gene flow events within each *C. pentheri* lineage but not between species (Fig. 10A). The F_b tests (Fig. 10B) revealed three significant admixture events. In *C. pentheri pentheri*, one admixture event was inferred between the ancestors of

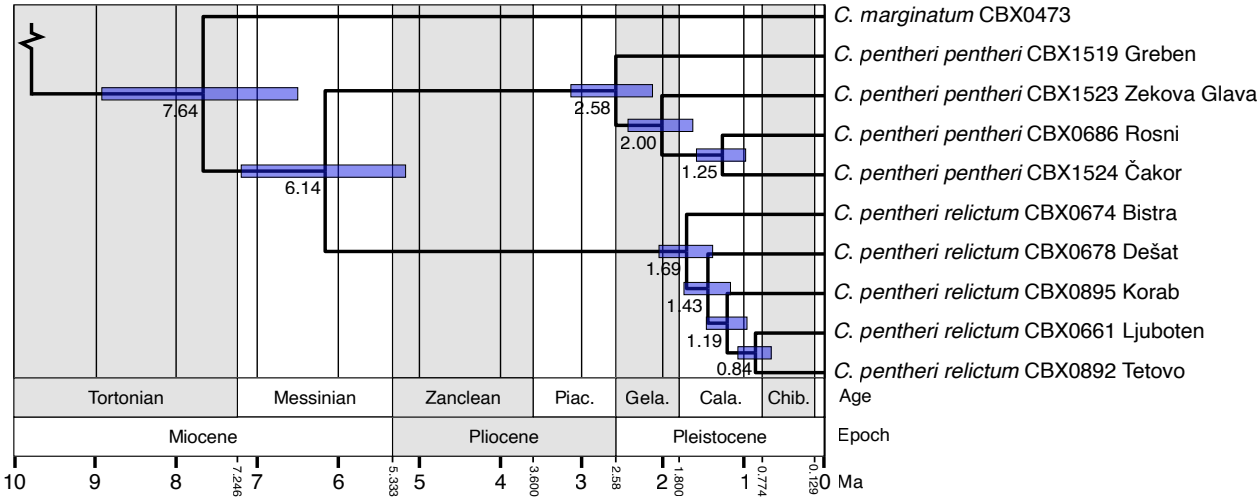

Figure 9. Divergence estimate tree. Time-calibrated tree of *Calosoma pentheri* lineages generated in BEAST using a reduced genomic dataset, eight partitions and under a coalescent constant population size tree model (replicate 1 is presented here). Node bars indicate the 95% highest posterior density (HPD) intervals while nodes represent median age estimates. Chronometric epochs and ages are shown along the x-axis, with start and end points indicated. Abbreviated epochs include Piacenzian, Gelasian, Calabrian, and Chibanian. The complete tree topology is provided in Suppl. material 2.

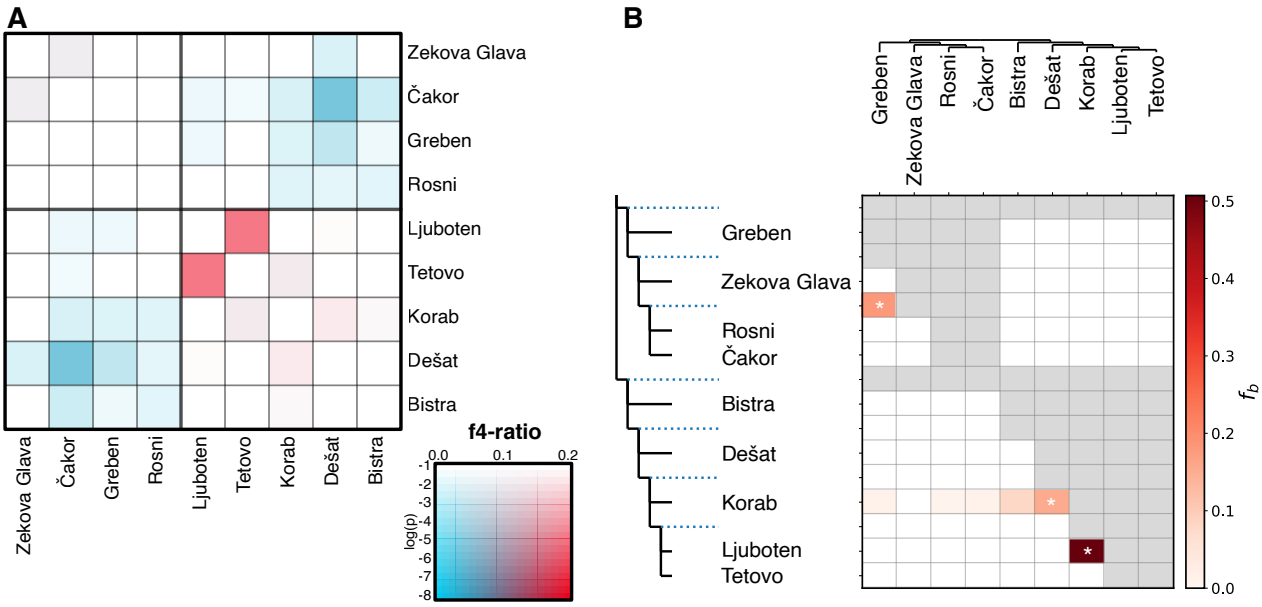

Figure 10. Introgression analysis within *C. pentheri* lineages. Introgression analyses visualized using Dsuite showing (**A**) F4-ratio results and (**B**) F_b method results. In both plots, color and oppacity represents the degree of admixture, with increased oppacity indicating higher admixture estimates. In **panel B**, gray cells denote tests not applicable based on the phylogeny, and asterisks (*) mark F_b estimates with a z-score ≥ 3. Figures were stylized and annotated in Inkscape.

Rosni + Čakor and Greben localities. In *C. pentheri relictum*, two admixture events were inferred: one between Lujboten and Korab, and another between Korab and Dešat.

Discussion

Phylogenetic relationships, population genomics and taxonomic implications

Our phylogenomic analyses recovered *Calosoma pentheri sensu lato* as sister to *C.* (*Callisthenes*) *marginatum*, with strong branch support (Fig. 8). This placement is in line with the current classification of *C. pentheri sensu lato* as a member of the subgenus *Callisthenes* (Obydov 2002; Bruschi 2013). Additional taxon sampling within this group would be important to clarify the precise placement of *C. pentheri sensu lato* relative to other closely related species, both geographically and morphologically. Nevertheless, the affinity of *C. pentheri sensu lato* with *C. marginatum* had already been highlighted based on convergent genitalic structures (Obydov 2002). Furthermore, these two lineages are the geographically closest among *Callisthenes*, despite a large disjunct distribution between the Western Balkans and Kazakhstan where *C. marginatum* occurs (Obydov 2002; Bruschi 2013). The sister relationship of *Callisthenes* with *Callistenia* is also of interest as it was already suggested by previous studies (Su et al. 2005; Sota et al. 2022; Cardenas et al. 2025). The affinities of these two subgenera are in line with the historical hypothesis of René Jeannel (1940) who proposed to lump parts of these two genera into the subgenus *Microcallisthenes*. However, the placement of *Callisthenes* and *Callistenia* within the genus *Calosoma*, their reciprocal monophyly and their relationship with the subgenus *Chrysostigma* Kirby, 1837 remain largely untested. Two previous molecular studies suggested that species within *Callistenia* and *Callisthenes* could be mixed into a larger clade (Toussaint and Gillett 2018; Sota et al. 2022), lending some additional support to the scenario of Jeannel (1940). Reconstructing the phylogenetic placement of *C. pentheri sensu lato* with respect to other morphologically closely-related species in the subgenus *Callistenia*, such as *C. moniliatum* LeConte, 1852, would be interesting to understand the evolutionary history of those trans-Beringian lineages. However, these hypotheses remain to be investigated at a larger-scale using a comprehensive taxon sampling across Holarctic *Calosoma* subgenera.

Within *C. pentheri sensu lato*, we recovered well-defined geographic clades corresponding to major mountain ranges, illustrating a strong paleogeographic signature at the genomic level. In regions where the geography is more contiguous, such as Montenegro and northern Albania, we identified a single population of *C. pentheri pentheri*. A different pattern was observed in *C. pentheri relictum* in which Bistra populations are more geographically isolated from other populations in North Macedonia. The remaining populations of *C. pentheri relictum* are found on a more or less continuous series of mountains along the border between North Macedonia, Albania and Kosovo because they are well connected with almost unfragmented mountain pastures. This geographic continuity was reflected in uncertainty regarding the relationships of the Northwestern sites in the ML phylogenetic analyses. However, a more obvious geographic barrier exists between *C. pentheri pentheri* and *C. pentheri relictum*. The mountains in Albania separating Montenegro and North Macedonia do not reach 2000 m, and thus lack suitable habitat to host either lineage of *C. pentheri sensu lato*, and this is reflected in our phylogenetic analyses. These phylogenomic inferences are largely confirmed by the population genomic results. The STRUCTURE analyses support a scenario with two evolutionarily independent lineages as illustrated by a DeltaK = 2, with no signal of recent hybridization. This suggests that genomic segregation between the two subspecies is near complete. In contrast, both show evidence of recent admixture or introgression within their respective lineages, as evidenced by signatures of gene flow (Fig. 10B). These admixture events likely occurred during glacial maxima in the Pleistocene (Adamson et al. 2013).

Divergence time estimations recovered an origin of *C. pentheri sensu lato* in the Late Miocene with modern lineages originating *ca.* 6 Ma (95% credibility interval: 5.15–7.18 Ma), indicating that the split between these two lineages largely predated glaciation cycles from the Plio-Pleistocene. Integrating the above results clearly indicates that the two current subspecies of *C. pentheri* should be considered distinct species. This is largely in line with the morphological studies of Jeannel (1940) and Obydov (2002). Since Bruschi (2013) did not formally synonymize the two species, there is no nomenclatural act to be performed, but future work should regard *C. pentheri* and *C. relictum* as *bona species*, and those are treated as such hereafter. Considering the strong geographical and genomic structure among *C. relictum* populations, a more in-depth investigation of morphological variation could support the future description of new subspecies within this lineage. Earlier studies proposed such subspecific delineation based on subtle morphological differences (Roubal 1932; Breuning 1977), but careful reexamination of said features demonstrates that these are more pervasive than originally believed, and the new taxa are now considered synonyms (Obydov 2002; Bruschi 2013; this study). Future work should ideally encompass both fine-scale population genomic analyses across the entire range of *C. relictum*, and detailed morphometric analyses including both external and genitalic features allowing for the discrimination of consistent morphological divergences, if any.

Evolutionary history of *Calosoma* beetles in Western Balkan highlands

Both *C. pentheri* and *C. relictum* exhibit clear allopatry, as shown by their disjunct distribution in lowlands between western Kosovo and the mid-elevation mountains (<1800 m) of western Albania. In this intermediate region, the highest peaks, Maja e Malit (1683 m), Maja e Midës (1682 m) and Maja e Muleqithit (1735 m), are below the

elevation needed to host these alpine species. This topography, however, already existed when both lineages diverged *ca.* 5–7 Ma (Northern Albanides >17 Ma, see Muceku et al. 2006, 2008; Mazzoli et al. 2022). During colder periods, such as glacial maxima, it is likely that these lower elevation mountain ranges harbored alpine biotopes resembling those currently occupied by *C. pentheri* and *C. relictum* (typically >2000 m). The absence of evidence of recent admixture between these two species suggests that gene flow ceased long before the onset of Quaternary glaciations *ca.* 2.6 Ma. These observations support an evolutionary scenario largely shaped by climatic shifts in the Neogene.

We hypothesize that the ancestor of both species likely occurred in the entire range currently occupied by both species during the Late Miocene, when progressive global cooling *ca.* 7 Ma (Herbert et al. 2016; Steinthorsdottir et al. 2021) would have allowed a wider ancestral range in glacial refugia such as the above-mentioned mid-elevation ranges between northern Accursed Mountains and the Korab massif (Fig. 11). In the next stage, as global

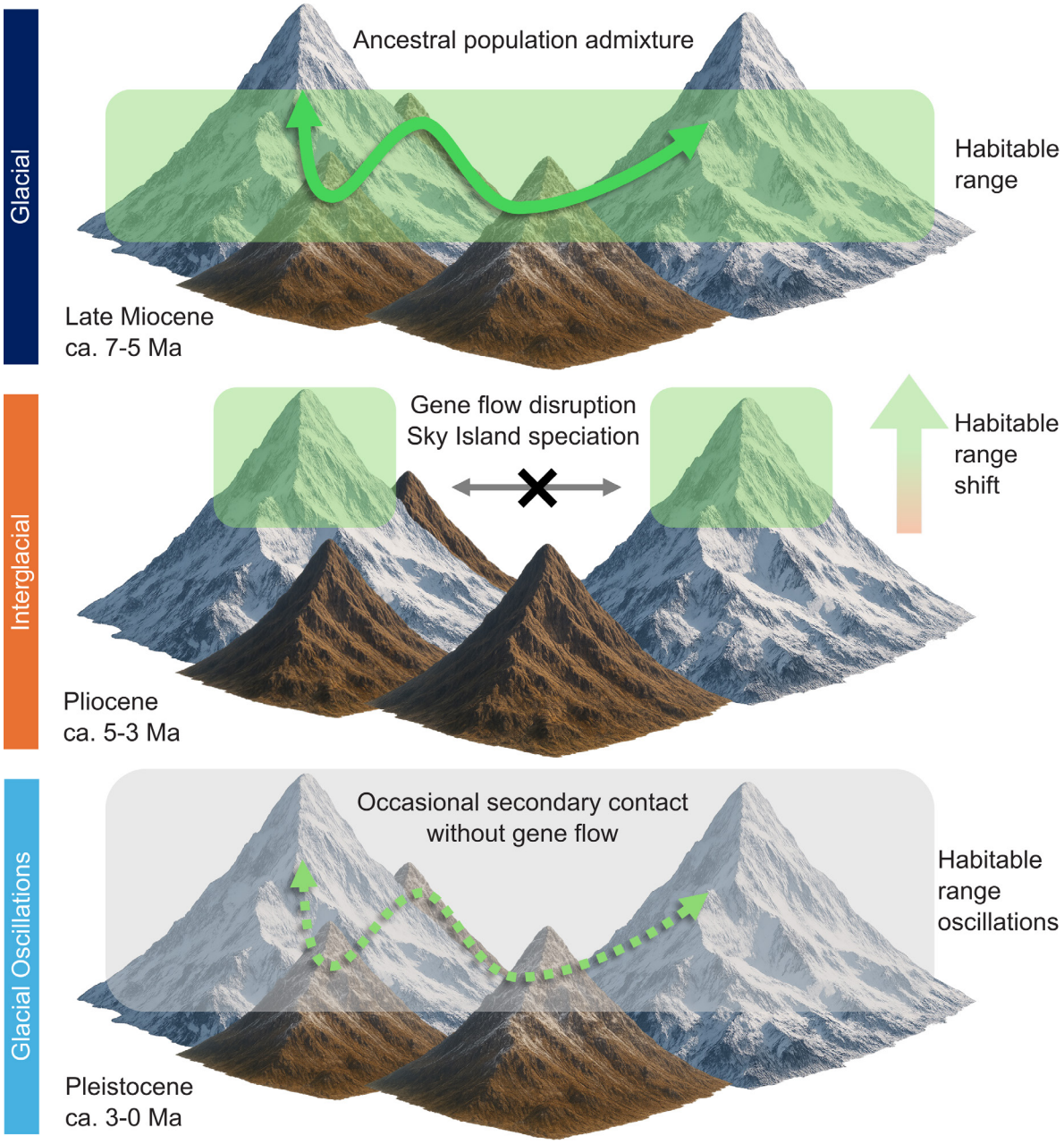

Figure 11. Evolutionary hypothesis of *C. pentheri* and *C. relictum* in the Western Balkans. Figure illustrating the proposed evolutionary scenario underlying the allopatric speciation of *C. pentheri* and *C. relictum*. The figure is divided into three rows, with the top row depicting a cold, glaciated period in the Late Miocene. A hypothetical ancestral range is shown in green indicating continuous connectivity between mountain ranges that allowed gene flow. The middle row depicts a warmer interglacial period in the Pliocene. Here, the ancestral range contracted to higher elevations as lower mountains became inhospitable, disrupting gene flow between the two ranges. The bottom row illustrates Pleistocene glacial oscillations, during which range restrictions fluctuated and intermittent connectivity allowed occasional secondary contact between the two ranges, but without gene flow.

climate warmed progressively between the Late Miocene and the Pliocene Thermal Maximum (Lunt et al. 2012; Haywood et al. 2016), these ephemeral refugia became inhospitable (i.e., too warm) and both lineages may have dispersed to higher elevations in alpine massifs on each side of the ancestral range (i.e., their current altitudinal ranges). These alpine refugia functioned as isolated mountain ranges, or "sky islands" (Smith and Farrell 2005; McCormack et al. 2009; Toussaint et al. 2013; Chou et al. 2021; Love et al. 2023) with no opportunity for dispersal in brachypterous flightless species such as *C. pentheri* and *C. relictum*. Divergence time estimates indicate that both species split *ca.* 5–7 Ma, coinciding with the peak and conclusion of the Late Miocene cooling event *ca.* 5.4–7 Ma (Herbert et al. 2016). These estimated ages of cladogenesis are consistent with a postglacial evolutionary scenario, in which progressively warmer climatic conditions possibly triggered allopatric isolation, resulting in incipient speciation (Robin et al. 2010; Suzuki et al. 2024). Consequently, both lineages remained confined to higher-elevation biotopes (i.e., sky islands) until the end of the Pliocene Thermal Maximum, allowing complete allopatric speciation (Carstens and Knowles 2007; Schoville et al. 2012; Ortego and Knowles 2022). In the subsequent stage, Pleistocene glaciations began long after speciation had concluded, with possible secondary contact in the same mid-elevation glacial refugia, but this time without gene flow due to complete genetic sorting. Although secondary contact may have occurred, it was likely limited due to high ELAs, deeply dissected mountainous relief, and fragmentated grassland habitats in the Western Balkans. Finally, a second episode of postglacial climate-driven allopatry likely established the present-day disjunct geographic ranges of these species across the Western Balkans.

Glacial refugia that preserved lineages during a global cooling period have been well documented (Hewitt 1996; Carstens and Knowles 2007; Bennett and Provan 2008; Stewart et al. 2010). Temperate species often contract their range into scattered refugia during peak glacial periods, and during interglacial periods their ranges expand (Hewitt 2004). These processes of range contraction and expansion drive powerful evolutionary forces such as genetic drift, geographic isolation, and local adaptation which can lead to diversification and extinction events. In contrast, some cold-adapted species experience range contractions during interglacial periods (Stewart et al. 2010), as observed in Anatolian ground squirrels (*Spermophilus*; Gür 2013), West Palearctic bumblebees (*Bombus*; Martinet et al. 2018), North American beardtongue flowers (*Penstemon*; Stone and Wolfe 2021), and Chinese scorpionflies (*Cerapanorpa*; Gao et al. 2022). Our study provides another example of this pattern, with endemic ground beetles adapted to cool and dry Western Balkan mountains, whose ranges likely expanded during glacial maxima and contracted during interglacial periods, thereby driving allopatric speciation. Given the pace of global climate change (Bellard et al. 2012), the same processes of range contraction that drove these evolutionary patterns could now result in the extinction of flora and fauna in sky island archipelagoes (Freeman et al. 2018; Yanahan and Moore 2019; Monroy-Gamboa et al. 2022; Love et al. 2023). Western Balkan sky islands are at risk given that many of the localities we sampled are at or near the altitudinal limits of these mountains. The highest summits in the Accursed Mountains where *Calosoma pentheri* occurs reach *ca.* 2500 m, while in Šar Mountains where *C. relictum* is found, the highest summits reach *ca.* 2700 m. Further range contraction fueled by global warming (Gulev et al. 2021; Intergovernmental Panel On Climate Change 2021), would lead to the unequivocal extinction of many sky island lineages in the long term. The fine-scale biogeographic processes observed for *Calosoma pentheri* and *C. relictum* likely occur in other endemic lineages of the Western Balkans. It is likely that entire endemic sky island communities will face similar levels of threats in the foreseeable future.

Conclusion

Our genomic analyses support a clear delineation between *Calosoma pentheri* and *C. relictum*, confirming earlier hypotheses regarding species boundaries. These analyses, in combination with divergence time estimations, suggest that global warming between the Late Miocene and Pliocene likely triggered speciation between *C. pentheri* and *C. relictum* in Western Balkan sky islands. Subsequent Quaternary glaciations occurred after genetic sorting and possible secondary contact between the two species did not result in admixture. On each side of the Western Balkan highlands, populations of the two species also evolved in response to ice ages but in different manners. In the north, current populations of *C. pentheri* display low levels of genomic divergences likely due to the continuous landscape of the Accursed Mountains. In contrast, populations of *C. relictum* present a more structured fine-scale genomic landscape explained by a more dissected geological setup. These results indicate that both lineages dynamically responded to past climate shifts, however their current habitats along some of the highest elevational gradients of Western Balkan mountains are threatened by global warming. More broadly, cold-adapted species occurring close to summits are likely to face immediate threats in the context of ongoing global warming. Future research should focus on assessing the resilience of such lineages to future climatic oscillations and potentially rely on habitat suitability modeling to inform conservation policies.

Acknowledgements

We want to thank Marie Pauli and Marjan Komnenov for assistance in fieldwork campaigns. We are also grateful to all curators that allowed access to samples; Michael Balke (SNSB-ZSM), Mathias Borer (NMBS), Arnaud Faille (SMNS), Anne Freitag (Naturéum), and Matthias Seidel (NHM Wien).

Funding

This study was funded by a Swiss National Science Foundation grant 310030_200491 to Emmanuel F.A. Toussaint. Permit for scientific research in nature, issued by the Ministry of Environment and Physical Planning of the Republic of North Macedonia, Nr. UP1-11/1-180/2022 from 11.03.2022

Author contributions

CRC, SH and EFAT conceptualized this study. CRC, SH and EFAT contributed the sampling. CRC, JG, HM and JB curated the data, developed the methodology and led the analyses. CRC and EFAT drafted the original manuscript, tables and figures. JG, HM, JB and SH contributed to the writing and editing of the finalized manuscript. SH and EFAT contributed to the project administration and resources.

Artificial Intelligence (AI) use

The authors accept full responsibility for the content of the manuscript: no AI tools were used in the writing, coding, or analysis of data.

Data Availability

Custom scripts used are available from: https://github.com/crcardenas/Balkans_calosoma;
NCBI Project Accession: PRJNA1390611;
Genome accession number GCA_055275695.1;
Supplemental Data: https://doi.org/10.5281/zenodo.18107202.

References

Adamson KR, Hughes P, Woodward J (2013) Pleistocene glaciation of the Mediterranean Mountains. Quaternary Newsletter 131: 2–15.

Apfelbeck V (1918) Koleopteren aus dem nordalbanisch-montenegrinischen Grenzgebiete (Ergebnisse einer von der Kaiserl. Akademie der Wissenschaften in Wien veranlaßten naturwissenschaftlichen Forschungsreise in Nordabanien). Sitzungsberichte der Kaiserlichen Akademie der Wissenschaften. Mathematisch-Naturwissenschaftliche Klasse. Abt. 3, Anatomie und Physiologie des Menschen und der Tiere sowie aus jenem der theoretischen Medizin 127: 159–176.

Araújo MB, Rahbek C (2006) How does climate change affect biodiversity? Science 313: 1396–1397. https://doi.org/10.1126/science.1131758

Barnosky AD, Hadly EA, Gonzalez P, Head J, Polly PD, Lawing AM, Eronen JT, Ackerly DD, Alex K, Biber E, Blois J, Brashares J, Ceballos G, Davis E, Dietl GP, Dirzo R, Doremus H, Fortelius M, Greene HW, Hellmann J, Hickler T, Jackson ST, Kemp M, Koch PL, Kremen C, Lindsey EL, Looy C, Marshall CR, Mendenhall C, Mulch A, Mychajliw AM, Nowak C, Ramakrishnan U, Schnitzler J, Das Shrestha K, Solari K, Stegner L, Stegner MA, Stenseth NChr, Wake MH, Zhang Z (2017) Merging paleobiology with conservation biology to guide the future of terrestrial ecosystems. Science 355: eaah4787. https://doi.org/10.1126/science.aah4787

Bellard C, Bertelsmeier C, Leadley P, Thuiller W, Courchamp F (2012) Impacts of climate change on the future of biodiversity. Ecology Letters 15: 365–377. https://doi.org/10.1111/j.1461-0248.2011.01736.x

Bennett K, Provan J (2008) What do we mean by 'refugia'? Quaternary Science Reviews 27: 2449–2455. https://doi.org/10.1016/j.quascirev.2008.08.019

Borowiec ML (2016) AMAS: a fast tool for alignment manipulation and computing of summary statistics. PeerJ 4: e1660. https://doi.org/10.7717/peerj.1660

Breuning S (1977) Description de nouvelles races des genres *Calosoma* Web. et *Carabus* L. Bulletin de la Societe Entomologique de Mulhouse 48: 81–141. https://www.zobodat.at/pdf/WEZ_44_0081-0141.pdf

Broad Institute (2019) Picard Toolkit. https://broadinstitute.github.io/picard/

Brown JW, Walker JF, Smith SA (2017) Phyx: phylogenetic tools for unix. ed. by J. Kelso. Bioinformatics 33: 1886–1888. https://doi.org/10.1093/bioinformatics/btx063

Bruschi S (2013) *Calosoma* of the world: (Coleoptera, Carabidae). Natura edizioni scientifiche, Bologna (Italy).

Capella-Gutiérrez S, Silla-Martínez JM, Gabaldón T (2009) trimAl: a tool for automated alignment trimming in large-scale phylogenetic analyses. Bioinformatics 25: 1972–1973. https://doi.org/10.1093/bioinformatics/btp348

Cardenas CR, Gustafson G, Toussaint E (2025) Global integration of phylogenomic data and fine-scale partitioning strategies refine the evolutionary tree of Adephaga beetles. Bulletin of the Society of Systematic Biologists 4. https://doi.org/10.18061/bssb.v4i1.10345

Carstens BC, Knowles LL (2007) Shifting distributions and speciation: species divergence during rapid climate change. Molecular Ecology 16: 619–627. https://doi.org/10.1111/j.1365-294X.2006.03167.x

Casale A, Vigna Taglianti A (1999) Caraboid beetles (excl. Cicindelidae) of Anatolia, and their biogeographical significance (Coleoptera, Caraboidea). Biogeographia – The Journal of Integrative Biogeography 20: 277–407. https://doi.org/10.21426/B620110002

Challis R, Richards E, Rajan J, Cochrane G, Blaxter M (2020) BlobToolKit – Interactive Quality Assessment of Genome Assemblies. G3 Genes|Genomes|Genetics 10: 1361–1374. https://doi.org/10.1534/g3.119.400908

Chen S, Zhou Y, Chen Y, Gu J (2018) fastp: an ultra-fast all-in-one FASTQ preprocessor. Bioinformatics 34: i884–i890. https://doi.org/10.1093/bioinformatics/bty560

Cheng H, Concepcion GT, Feng X, Zhang H, Li H (2021) Haplotype-resolved de novo assembly using phased assembly graphs with hifiasm. Nature Methods 18: 170–175. https://doi.org/10.1038/s41592-020-01056-5

Chernomor O, Von Haeseler A, Minh BQ (2016) Terrace aware data structure for Phylogenomic inference from supermatrices. Systematic Biology 65: 997–1008. https://doi.org/10.1093/sysbio/syw037

Chou MH, Tseng WZ, Sang YD, Morgan B, De Vivo M, Kuan YH, Wang LJ, Chen WY, Huang JP (2021) Incipient speciation and its impact on taxonomic decision: a case study using a sky island sister-species pair of stag beetles (Lucanidae: *Lucanus*). Biological Journal of the Linnean Society 134: 745–759. https://doi.org/10.1093/biolinnean/blab105

Clark L (2017) lvclark/R_genetics_conv: R_genetics_conv 1.1. https://doi.org/10.5281/ZENODO.846816

Danecek P, Auton A, Abecasis G, Albers CA, Banks E, DePristo MA, Handsaker RE, Lunter G, Marth GT, Sherry ST, McVean G, Durbin R, 1000 Genomes Project Analysis Group (2011) The variant call format and VCFtools. Bioinformatics 27: 2156–2158. https://doi.org/10.1093/bioinformatics/btr330

Davis MB, Shaw RG (2001) Range shifts and adaptive responses to Quaternary Climate Change. Science 292: 673–679. https://doi.org/10.1126/science.292.5517.673

Dawson TP, Jackson ST, House JI, Prentice IC, Mace GM (2011) Beyond predictions: Biodiversity conservation in a changing climate. Science 332: 53–58. https://doi.org/10.1126/science.1200303

Fedorov AV, Brierley CM, Lawrence KT, Liu Z, Dekens PS, Ravelo AC (2013) Patterns and mechanisms of early Pliocene warmth. Nature 496: 43–49. https://doi.org/10.1038/nature12003

Fonseca EM, Pelletier TA, Decker SK, Parsons DJ, Carstens BC (2023) Pleistocene glaciations caused the latitudinal gradient of within-species genetic diversity. Evolution Letters 7: 331–338. https://doi.org/10.1093/evlett/qrad030

Foster LC, Schmidt DN, Thomas E, Arndt S, Ridgwell A (2013) Surviving rapid climate change in the deep sea during the Paleogene hyperthermals. Proceedings of the National Academy of Sciences 110: 9273–9276. https://doi.org/10.1073/pnas.1300579110

Francis RM (2017) pophelper: an R package and web app to analyse and visualize population structure. Molecular Ecology Resources 17: 27–32. https://doi.org/10.1111/1755-0998.12509

Freeman BG, Lee Yaw JA, Sunday JM, Hargreaves AL (2018) Expanding, shifting and shrinking: The impact of global warming on species' elevational distributions. Global Ecology and Biogeography 27: 1268–1276. https://doi.org/10.1111/geb.12774

Gao K, Hua Y, Xing L-X, Hua B-Z (2022) Speciation of the cold-adapted scorpionfly *Cerapanorpa brevicornis* (Mecoptera: Panorpidae) via interglacial refugia. Insect Conservation and Diversity 15: 114–127. https://doi.org/10.1111/icad.12519

Gauthier J, Pajkovic M, Neuenschwander S, Kaila L, Schmid S, Orlando L, Alvarez N (2020) Museomics identifies genetic erosion in two butterfly species across the 20th century in Finland. Molecular Ecology Resources 20: 1191–1205. https://doi.org/10.1111/1755-0998.13167

Gauthier J, Borer M, Toussaint EFA, Bilat J, Kippenberg H, Alvarez N (2023) Museomics reveals evolutionary history of *Oreina* alpine leaf beetles (Coleoptera: Chrysomelidae). Systematic Entomology 48: 658–671. https://doi.org/10.1111/syen.12601

Gauthier J, Blanc M, Toussaint EFA (2025a) Chromosome-scale genomes of the flightless Caterpillar Hunter Beetles *Calosoma tepidum* and *Calosoma wilkesii* from British Columbia (Coleoptera: Carabidae). Genome Biology and Evolution 17: evae247. https://doi.org/10.1093/gbe/evae247

Gauthier J, Cardenas CR, Nari M, Gillett CPDT, Toussaint EFA (2025b) Draft genome of the endemic alpine ground beetle *Carabus* (*Platycarabus*) *depressus* (Coleoptera: Carabidae) from long-read sequencing of a frozen archived specimen. ed. by E. J J. G3: Genes, Genomes, Genetics: jkaf027. https://doi.org/10.1093/g3journal/jkaf027

Goudet J (2005) hierfstat, a package for R to compute and test hierarchical F-statistics. Molecular Ecology Notes 5: 184–186. https://doi.org/10.1111/j.1471-8286.2004.00828.x

Grabowski M, Mamos T, Bącela-Spychalska K, Rewicz T, Wattier RA (2017) Neogene paleogeography provides context for understanding the origin and spatial distribution of cryptic diversity in a widespread Balkan freshwater amphipod. PeerJ 5: e3016. https://doi.org/10.7717/peerj.3016

Griffiths HI, Kryštufek B, Reed JM [Eds] (2004) Balkan Biodiversity. Springer Netherlands, Dordrecht. https://doi.org/10.1007/978-1-4020-2854-0

Grimm NB, Chapin FS, Bierwagen B, Gonzalez P, Groffman PM, Luo Y, Melton F, Nadelhoffer K, Pairis A, Raymond PA, Schimel J, Williamson CE (2013) The impacts of climate change on ecosystem structure and function. Frontiers in Ecology and the Environment 11: 474–482. https://doi.org/10.1890/120282

Gross R, Lovrenčić L, Jelić M, Grandjean F, Đuretanović S, Simić V, Burimski O, Bonassin L, Groza MI, Maguire I (2021) Genetic diversity and structure of the noble crayfish populations in the Balkan Peninsula revealed by mitochondrial and microsatellite DNA markers. PeerJ 9: e11838. https://doi.org/10.7717/peerj.11838

Guan D, McCarthy SA, Wood J, Howe K, Wang Y, Durbin R (2020) Identifying and removing haplotypic duplication in primary genome assemblies. ed. by A. Valencia. Bioinformatics 36: 2896–2898. https://doi.org/10.1093/bioinformatics/btaa025

Guéorguiev B (2007) Biogeography of the Endemic Carabidae (Coleoptera) in the Central and Eastern Balkan Peninsula. In: Fet V, Popov A (Eds) Biogeography and Ecology of Bulgaria, Springer Netherlands, Dordrecht, 297–356. https://doi.org/10.1007/978-1-4020-5781-6_9

Guindon S, Dufayard JF, Lefort V, Anisimova M, Hordijk W, Gascuel O (2010) New algorithms and methods to estimate maximum-likelihood phylogenies: assessing the performance of PhyML 3.0. Systematic Biology 59: 307–321. https://doi.org/10.1093/sysbio/syq010

Gulev S, Thorne P, Ahn J, Dentener F, Domingues C, Gerland S, Gong D, Kaufman D, Nnamchi H, Quaas J, Rivera J, Sathyendranath S, Smith S, Trewin B, Schuckmann K, Vose R (2021) IPCC AR6 WGI Chapter 2: Changing state of the climate system.

Gür H (2013) The effects of the Late Quaternary glacial-interglacial cycles on Anatolian ground squirrels: range expansion during the glacial periods? Biological Journal of the Linnean Society 109: 19–32. https://doi.org/10.1111/bij.12026

Haywood AM, Valdes PJ (2004) Modelling Pliocene warmth: contribution of atmosphere, oceans and cryosphere. Earth and Planetary Science Letters 218: 363–377. https://doi.org/10.1016/S0012-821X(03)00685-X

Haywood AM, Dowsett HJ, Dolan AM (2016) Integrating geological archives and climate models for the mid-Pliocene warm period. Nature Communications 7: 10646. https://doi.org/10.1038/ncomms10646

Herbert TD, Lawrence KT, Tzanova A, Peterson LC, Caballero-Gill R, Kelly CS (2016) Late Miocene global cooling and the rise of modern ecosystems. Nature Geoscience 9: 843–847. https://doi.org/10.1038/ngeo2813

Hewitt G (1996) Some genetic consequences of ice ages, and their role in divergence and speciation. Biological Journal of the Linnean Society 58: 247–276. https://doi.org/10.1006/bijl.1996.0035

Hewitt GM (2004) Genetic consequences of climatic oscillations in the Quaternary. ed. by K.J. Willis, K.D. Bennett, and D. Walker. Philosophical Transactions of the Royal Society of London. Series B: Biological Sciences 359: 183–195. https://doi.org/10.1098/rstb.2003.1388

Hijmans RJ (2019) Geosphere: spherical trigonometry. R package.

Hoang DT, Chernomor O, von Haeseler A, Minh BQ, Vinh LS (2018) UFBoot2: improving the ultrafast bootstrap approximation. Molecular Biology and Evolution 35: 518–522. https://doi.org/10.1093/molbev/msx281

Holmes J, Lowe J, Wolff E, Srokosz M (2011) Rapid climate change: lessons from the recent geological past. Global and Planetary Change 79: 157–162. https://doi.org/10.1016/j.gloplacha.2010.10.005

Hristovski S, Guéorguiev B (2015) Annotated catalogue of the carabid beetles of the Republic of Macedonia (Coleoptera: Carabidae). Zootaxa 4002: 1–190. https://doi.org/10.11646/zootaxa.4002.1.1

Hristovski S, Mihajlova B, Guéorguiev B (2016) Review of the ground beetles (Coleoptera, Carabidae) from Macedonia in the collection of the Macedonian Museum of Natural History.

Hughes PD (2010) Little Ice Age glaciers in the Balkans: low altitude glaciation enabled by cooler temperatures and local topoclimatic controls. Earth Surface Processes and Landforms 35: 229–241. https://doi.org/10.1002/esp.1916

Hughes TP, Kerry JT, Baird AH, Connolly SR, Dietzel A, Eakin CM, Heron SF, Hoey AS, Hoogenboom MO, Liu G, McWilliam MJ, Pears RJ, Pratchett MS, Skirving WJ, Stella JS, Torda G (2018) Global warming transforms coral reef assemblages. Nature 556: 492–496. https://doi.org/10.1038/s41586-018-0041-2

Inkscape Project (2025) Inkscape.

Intergovernmental Panel On Climate Change [IPCC] (2021) Climate Change 2021 – The Physical Science Basis: Working Group I Contribution to the Sixth Assessment Report of the Intergovernmental Panel on Climate Change. 1st ed.,. Cambridge University Press. https://doi.org/10.1017/9781009157896

Ivanov D, Utescher T, Mosbrugger V, Syabryaj S, Djordjević-Milutinović D, Molchanoff S (2011) Miocene vegetation and climate dynamics in Eastern and Central Paratethys (Southeastern Europe). Palaeogeography, Palaeoclimatology, Palaeoecology 304: 262–275. https://doi.org/10.1016/j.palaeo.2010.07.006

Jeannel R (1940) Les Calosomes. Mémoires du Muséum national d'histoire naturelle 13: 1–240.

Jombart T (2008) adegenet: a R package for the multivariate analysis of genetic markers. Bioinformatics 24: 1403–1405. https://doi.org/10.1093/bioinformatics/btn129

Jombart T, Ahmed I (2011) adegenet 1.3-1: new tools for the analysis of genome-wide SNP data. Bioinformatics 27: 3070–3071. https://doi.org/10.1093/bioinformatics/btr521

Jónsson H, Ginolhac A, Schubert M, Johnson PLF, Orlando L (2013) mapDamage2.0: fast approximate Bayesian estimates of ancient DNA damage parameters. Bioinformatics 29: 1682–1684. https://doi.org/10.1093/bioinformatics/btt193

Kalyaanamoorthy S, Minh BQ, Wong TKF, Von Haeseler A, Jermiin LS (2017) ModelFinder: fast model selection for accurate phylogenetic estimates. Nature Methods 14: 587–589. https://doi.org/10.1038/nmeth.4285

Katoh K, Standley DM (2013) MAFFT multiple sequence alignment software version 7: Improvements in performance and usability. Molecular Biology and Evolution 30: 772–780. https://doi.org/10.1093/molbev/mst010

Knaus BJ, Grünwald NJ (2016) VcfR: a package to manipulate and visualize VCF format data in R. https://doi.org/10.1101/041277

Knaus BJ, Grünwald NJ (2017) VCFR: a package to manipulate and visualize variant call format data in R. Molecular Ecology Resources 17: 44–53. https://doi.org/10.1111/1755-0998.12549

Krystufek B, Buzan EV, Hutchinson WF, Hänfling (2007) Phylogeography of the rare Balkan endemic Martino's vole, *Dinaromys bogdanovi*, reveals strong differentiation within the western Balkan Peninsula. Molecular Ecology 16: 1221–1232. https://doi.org/10.1111/j.1365-294X.2007.03235.x

Lanfear R, Frandsen PB, Wright AM, Senfeld T, Calcott B (2016) PartitionFinder 2: New methods for selecting partitioned models of evolution for molecular and morphological phylogenetic analyses. Molecular Biology and Evolution 34: 772–773. https://doi.org/10.1093/molbev/msw260

Li H, Durbin R (2009) Fast and accurate short read alignment with Burrows–Wheeler transform. Bioinformatics 25: 1754–1760. https://doi.org/10.1093/bioinformatics/btp324

Li H, Handsake, B, Wysoker A, Fennel, T, Ruan J, Homer N, Marth, G, Abecasis G, Durbin R, 1000 Genome Project Data Processing Subgroup (2009) The sequence alignment/map format and SAMtools. Bioinformatics 25: 2078–2079. https://doi.org/10.1093/bioinformatics/btp352

López-Moreno JI, García-Ruiz JM (2025) Discrepancies in dating the expansion of European glaciers during the Last Glacial Cycle. Geomorphology 471: 109566. https://doi.org/10.1016/j.geomorph.2024.109566

Love SJ, Schweitzer JA, Woolbright SA, Bailey J (2023) Sky islands are a global tool for predicting the ecological and evolutionary consequences of Climate Change. Annual Review of Ecology, Evolution, and Systematics 54: 219–236. https://doi.org/10.1146/annurev-ecolsys-102221-050029

Lunt DJ, Haywood AM, Schmidt GA, Salzmann U, Valdes PJ, Dowsett HJ, Loptson CA (2012) On the causes of mid-Pliocene warmth and polar amplification. Earth and Planetary Science Letters 321–322: 128–138. https://doi.org/10.1016/j.epsl.2011.12.042

Malinsky M, Matschine M, Svardal H (2021) Dsuite Fast *D* statistics and related admixture evidence from VCF files. Molecular Ecology Resources 21: 584–595. https://doi.org/10.1111/1755-0998.13265

Martinet B, Lecocq T, Brasero N, Biella P, Urbanová K, Valterová I, Cornalba M, Gjershaug JO, Michez D, Rasmont P (2018) Following the cold: geographical differentiation between interglacial refugia and speciation in the arcto alpine species complex *Bombus monticola* (Hymenoptera: Apidae). Systematic Entomology 43: 200–217. https://doi.org/10.1111/syen.12268

Mazzoli S, Basilici M, Spina V, Pierantoni P, Tondi E (2022) Space and time variability of detachment versus ramp dominated thrusting: Insights from the outer Albanides. Tectonics 41: e2022TC007274. https://doi.org/10.1029/2022TC007274

McCormack J, Huang H, Knowles L (2009) Sky Islands. Encyclopedia of Islands 4.

McKenna DD, Shin S, Ahrens D, Balke M, Beza-Beza C, Clarke DJ, Donath A, Escalona HE, Friedrich F, Letsch H, Liu S, Maddison D, Mayer C, Misof B, Murin PJ, Niehuis O, Peters RS, Podsiadlowski L, Pohl H, Scully ED, Yan EV, Zhou X, Ślipiński A, Beutel RG (2019) The evolution and genomic basis of beetle diversity. Proceedings of the National Academy of Sciences 116: 24729–24737. https://doi.org/10.1073/pnas.1909655116

Milivojević M, Menković L, Ćalić J (2008) Pleistocene glacial relief of the central part of Mt. Prokletije (Albanian Alps). Quaternary International 190: 112–122. https://doi.org/10.1016/j.quaint.2008.04.006

Minh BQ, Hahn MW, Lanfear R (2020) New Methods to Calculate Concordance Factors for phylogenomic datasets. ed. by M. Rosenberg. Molecular Biology and Evolution 37: 2727–2733. https://doi.org/10.1093/molbev/msaa106

Monroy-Gamboa AG, Cab-Sulub L, Álvarez-Castañeda ST (2022) Extinction of endemic taxa as a direct consequence of global climate change. Therya 13: 79–84. https://doi.org/10.12933/therya-22-1210

Morgan-Wall T (2018) rayshader: Create Maps and Visualize Data in 2D and 3D. https://doi.org/10.32614/cran.package.rayshader

Muceku B, Mascle GH, Tashko A (2006) First results of fission-track thermochronology in the Albanides. Geological Society, London, Special Publications 260: 539–556. https://doi.org/10.1144/GSL.SP.2006.260.01.23

Muceku B, Van Der Beek P, Bernet M, Reiners P, Mascle G, Tashko A (2008) Thermochronological evidence for Mio Pliocene late orogenic extension in the north eastern Albanides (Albania). Terra Nova 20: 180–187. https://doi.org/10.1111/j.1365-3121.2008.00803.x

Nazareno AG, Bemmels JB, Dick CW, Lohmann LG (2017) Minimum sample sizes for population genomics: an empirical study from an Amazonian plant species. Molecular Ecology Resources 17: 1136–1147. https://doi.org/10.1111/1755-0998.12654

Obydov D (2002) Révision du genre *Callisthenes*. Magellanes, Andrésy France.

Ortego J, Knowles LL (2022) Geographical isolation versus dispersal: Relictual alpine grasshoppers support a model of interglacial diversification with limited hybridization. Molecular Ecology 31: 296–312. https://doi.org/10.1111/mec.16225

Ortiz EM (2019) vcf2phylip v2.0: convert a VCF matrix into several matrix formats for phylogenetic analysis. https://doi.org/10.5281/zenodo.2540861

Osawa S, Su ZH, Imura Y (2004) Phylogeny and distribution of the subfamily Carabinae. In: Molecular Phylogeny and Evolution of Carabid Ground Beetles. Springer Japan, Tokyo, 25–32. https://doi.org/10.1007/978-4-431-53965-0_4

Paradis E (2010) pegas: an R package for population genetics with an integrated–modular approach. Bioinformatics 26: 419–420. https://doi.org/10.1093/bioinformatics/btp696

Parmesan C, Yohe G (2003) A globally coherent fingerprint of climate change impacts across natural systems. Nature 421: 37–42. https://doi.org/10.1038/nature01286

Pauls SU, Lumbsch HT, Haase P (2006) Phylogeography of the montane caddisfly *Drusus discolor*: evidence for multiple refugia and periglacial survival. Molecular Ecology 15: 2153–2169. https://doi.org/10.1111/j.1365-294X.2006.02916.x

Petrušev E (2021) Geological characteristics of the Republic of North Macedonia. Geologica Macedonica 35: 49–58. https://doi.org/10.46763/GEOL21351372049ep

Poplin R, Ruano-Rubio V, DePristo MA, Fennell TJ, Carneiro MO, Van Der Auwera GA, Kling DE, Gauthier LD, Levy-Moonshine A, Roazen D, Shakir K, Thibault J, Chandran S, Whelan C, Lek M, Gabriel S, Daly MJ, Neale B, MacArthur DG, Banks E (2017) Scaling accurate genetic variant discovery to tens of thousands of samples. boiRxiv. https://doi.org/10.1101/201178

Previšić A, Schnitzler J, Kučinić M, Graf W, Ibrahimi H, Kerovec M, Pauls SU (2014) Microscale vicariance and diversification of Western Balkan caddisflies linked to karstification. Freshwater Science 33: 250–262. https://doi.org/10.1086/674430

Pritchard JK, Stephens M, Donnelly P (2000) Inference of population structure using multilocus genotype data. Genetics 155: 945–959. https://doi.org/10.1093/genetics/155.2.945

Quinlan AR, Hall IM (2010) BEDTools: a flexible suite of utilities for comparing genomic features. Bioinformatics 26(6): 841–842. https://doi.org/10.1093/bioinformatics/btq033

R Core Team (2025) R: A language and environment for statistical computing.

Rambaut A, Drummond AJ, Xie D, Baele G, Suchard MA (2018) Posterior summarization in Bayesian phylogenetics using Tracer 1.7. ed. by E. Susko. Systematic Biology 67: 901–904. https://doi.org/10.1093/sysbio/syy032

Ravelo AC, Andreasen DH, Lyle M, Olivarez Lyle A, Wara MW (2004) Regional climate shifts caused by gradual global cooling in the Pliocene epoch. Nature 429: 263–267. https://doi.org/10.1038/nature02567

Revell LJ (2024) phytools 2.0: an updated R ecosystem for phylogenetic comparative methods (and other things). PeerJ 12: e16505. https://doi.org/10.7717/peerj.16505

Robin VV, Sinha A, Ramakrishnan U (2010) Ancient geographical gaps and paleo-climate shape the phylogeography of an endemic bird in the Sky Islands of Southern India. ed. by S. Gadagkar. PLOS ONE 5: e13321. https://doi.org/10.1371/journal.pone.0013321

Ronikier M, Zalewska-Gałosz J (2014) Independent evolutionary history between the Balkan ranges and more northerly mountains in *Campanula alpina* s.l. (Campanulaceae): Genetic divergence and morphological segregation of taxa. TAXON 63: 116–131. https://doi.org/10.12705/631.4

Ronikier M, Kuzmanović N, Lakušić D, Stevanoski I, Nikolov Z, Zimmermann NE (2023) High-mountain phylogeography in the Balkan Peninsula: isolation pattern in a species of alpine siliceous grasslands and its possible background. Alpine Botany 133: 101–115. https://doi.org/10.1007/s00035-023-00296-3

Roubal J (1932) Fragmente zur Koleopterenfaunistik des balkanischen Festlandes. Entomologischer Anzeiger 12: 18–19. https://www.zobodat.at/pdf/EntAnz_12_0018-0019.pdf

Ruszkiczay-Rüdiger Z, Kern Z, Temovski M, Madarász B, Milevski I, Braucher R (2020) Last deglaciation in the central Balkan Peninsula: Geochronological evidence from the Jablanica Mt. (North Macedonia). Geomorphology 351: 106985. https://doi.org/10.1016/j.geomorph.2019.106985

Scheffers BR, De Meester L, Bridge TCL, Hoffmann AA, Pandolfi JM, Corlett RT, Butchart SHM, Pearce-Kelly P, Kovacs KM, Dudgeon D, Pacifici M, Rondinini C, Foden WB, Martin TG, Mora C, Bickford D, Watson JEM (2016) The broad footprint of climate change from genes to biomes to people. Science 354: aaf7671. https://doi.org/10.1126/science.aaf7671

Schmid S, Genevest R, Gobet E, Suchan T, Sperisen C, Tinner W, Alvarez N (2017) HyRAD X, a versatile method combining exome capture and RAD sequencing to extract genomic information from ancient DNA. ed. by M. Gilbert. Methods in Ecology and Evolution 8: 1374–1388. https://doi.org/10.1111/2041-210X.12785

Schmitt T (2007) Molecular biogeography of Europe: Pleistocene cycles and postglacial trends. Frontiers in Zoology 4: 11. https://doi.org/10.1186/1742-9994-4-11

Schoville SD, Roderick GK, Kavanaugh DH (2012) Testing the 'Pleistocene species pump' in alpine habitats: lineage diversification of flightless ground beetles (Coleoptera: Carabidae: *Nebria*) in relation to altitudinal zonation: Alpine *Nebria* comparative phylogeography. Biological Journal of the Linnean Society 107: 95–111. https://doi.org/10.1111/j.1095-8312.2012.01911.x

Seppey M, Manni M, Zdobnov EM (2019) BUSCO: Assessing Genome Assembly and Annotation Completeness. In: Kollmar M (Ed.) Gene Prediction: Methods and Protocols. Springer, New York, NY, 227–245. https://doi.org/10.1007/978-1-4939-9173-0_14

Smith CI, Farrell BD (2005) Phylogeography of the longhorn cactus beetle *Moneilema appressum* LeConte (Coleoptera: Cerambycidae): was the differentiation of the Madrean sky islands driven by Pleistocene climate changes? Molecular Ecology 14: 3049–3065. https://doi.org/10.1111/j.1365-294X.2005.02647.x

Smith SA, Brown JW, Walker JF (2018) So many genes, so little time: A practical approach to divergence-time estimation in the genomic era. ed. by H. Escriva. PLOS ONE 13: e0197433. https://doi.org/10.1371/journal.pone.0197433

Sota T, Michio H, Clarke S, Gayane K, Hong-Bin L, Hiroshi I, Yasuoki T (2020) The origin of the giant ground beetle *Aplothorax burchelli* on St Helena Island. Biological Journal of the Linnean Society 131: 50–60. https://doi.org/10.1093/biolinnean/blaa093

Sota T, Takami Y, Ikeda H, Liang H, Karagyan G, Scholtz C, Hori M (2022) Global dispersal and diversification in ground beetles of the subfamily Carabinae. Molecular Phylogenetics and Evolution 167: 107355. https://doi.org/10.1016/j.ympev.2021.107355

Steinthorsdottir M, Coxall HK, de Boer AM, Huber M, Barbolini N, Bradshaw CD, Burls NJ, Feakins SJ, Gasson E, Henderiks J, Holbourn AE, Kiel S, Kohn MJ, Knorr G, Kürschner WM, Lear CH, Liebrand D, Lunt DJ, Mörs T, Pearson PN, Pound MJ, Stoll H, Strömberg CAE (2021) The Miocene: The Future of the Past. Paleoceanography and Paleoclimatology 36: e2020PA004037. https://doi.org/10.1029/2020PA004037

Stewart JR, Lister AM, Barnes I, Dalén L (2010) Refugia revisited: individualistic responses of species in space and time. Proceedings of the Royal Society B: Biological Sciences 277: 661–671. https://doi.org/10.1098/rspb.2009.1272

Stone BW, Wolfe AD (2021) Phylogeographic analysis of shrubby beardtongues reveals range expansions during the Last Glacial Maximum and implicates the Klamath Mountains as a hotspot for hybridization. Molecular Ecology 30: 3826–3839. https://doi.org/10.1111/mec.15992

Su Z-H, Imura Y, Osawa S (2005) Evolutionary history of Calosomina ground beetles (Coleoptera, Carabidae, Carabinae) of the world as deduced from sequence comparisons of the mitochondrial ND5 gene. Gene 360: 140–150. https://doi.org/10.1016/j.gene.2005.06.028

Suchan T, Pitteloud C, Gerasimova NS, Kostikova A, Schmid S, Arrigo N, Pajkovic M, Ronikier M, Alvarez N (2016) Hybridization Capture Using RAD Probes (hyRAD), a New Tool for Performing Genomic Analyses on Collection Specimens. ed. by L. Orlando. PLOS ONE 11: e0151651. https://doi.org/10.1371/journal.pone.0151651

Suchard MA, Lemey P, Baele G, Ayres DL, Drummond AJ, Rambaut A (2018) Bayesian phylogenetic and phylodynamic data integration using BEAST 1.10. Virus Evolution 4. https://doi.org/10.1093/ve/vey016

Suzuki H, Takenaka M, Tojo K (2024) Phylogeography of an insect inhabiting 'Sky Islands': the relationships among genetic structures and geographical characteristics, geohistorical characteristics, and cyclical climate changes. Biological Journal of the Linnean Society 141: 503–519. https://doi.org/10.1093/biolinnean/blad112

Sworobowicz L, Grabowski M, Mamos T, Burzyński A, Kilikowska A, Sell J, Wysocka A (2015) Revisiting the phylogeography of *Asellus aquaticus* in Europe: insights into cryptic diversity and spatiotemporal diversification. Freshwater Biology 60: 1824–1840. https://doi.org/10.1111/fwb.12613

Sworobowicz L, Mamos T, Grabowski M, Wysocka A (2020) Lasting through the ice age: The role of the proglacial refugia in the maintenance of genetic diversity, population growth, and high dispersal rate in a widespread freshwater crustacean. Freshwater Biology 65: 1028–1046. https://doi.org/10.1111/fwb.13487

Taberlet P, Fumagalli L, Wust Saucy A, Cosson J (1998) Comparative phylogeography and postglacial colonization routes in Europe. Molecular Ecology 7: 453–464. https://doi.org/10.1046/j.1365-294x.1998.00289.x

Toussaint EFA, Gillett CPDT (2018) Rekindling Jeannel's Gondwanan vision? Phylogenetics and evolution of Carabinae with a focus on *Calosoma* Caterpillar Hunter Beetles. Biological Journal of the Linnean Society 123: 191–207. https://doi.org/10.1093/biolinnean/blx128

Toussaint EFA, Sagata K, Surbakti S, Hendrich L, Balke M (2013) Australasian sky islands act as a diversity pump facilitating peripheral speciation and complex reversal from narrow endemic to widespread ecological supertramp. Ecology and Evolution 3: 1031–1049. https://doi.org/10.1002/ece3.517

Toussaint EFA, Gauthier J, Bilat J, Gillett CPDT, Gough HM, Lundkvist H, Blanc M, Muñoz-Ramírez CP, Alvarez N (2021) HyRAD-X exome capture museomics unravels giant ground beetle evolution. ed. by M. dos Reis. Genome Biology and Evolution 13: evab112. https://doi.org/10.1093/gbe/evab112

Urzi F, Šprem N, Potočnik H, Sindičić M, Konjević D, Ćirović D, Rezić A, Duniš L, Melovski D, Buzan E (2021) Population genetic structure of European wildcats inhabiting the area between the Dinaric Alps and the Scardo-Pindic mountains. Scientific Reports 11: 17984. https://doi.org/10.1038/s41598-021-97401-5

Vangestel C, Swaegers J, De Corte Z, Dekoninck W, Gharbi K, Gillespie R, Vandekerckhove M, Van Belleghem SM, Hendrickx F (2024) Chromosomal inversions from an initial ecotypic divergence drive a gradual repeated radiation of Galápagos beetles. Science Advances 10: eadk7906. https://doi.org/10.1126/sciadv.adk7906

Westerhold T, Marwan N, Drury AJ, Liebrand D, Agnini C, Anagnostou E, Barnet JSK, Bohaty SM, De Vleeschouwer D, Florindo F, Frederichs T, Hodell DA, Holbourn AE, Kroon D, Lauretano V, Littler K, Lourens LJ, Lyle M, Pälike H, Röhl U, Tian J, Wilkens RH, Wilson PA, Zachos JC (2020) An astronomically dated record of Earth's climate and its predictability over the last 66 million years. Science 369: 1383–1387. https://doi.org/10.1126/science.aba6853

Wickham H (2016) ggplot2. Springer International Publishing, Cham. https://doi.org/10.1007/978-3-319-24277-4

Wiens JJ, Zelinka J (2024) How many species will Earth lose to climate change? Global Change Biology 30: e17125. https://doi.org/10.1111/gcb.17125

Willis KJ, Bailey RM, Bhagwat SA, Birks HJB (2010) Biodiversity baselines, thresholds and resilience: testing predictions and assumptions using palaeoecological data. Trends in Ecology & Evolution 25: 583–591. https://doi.org/10.1016/j.tree.2010.07.006

Yanahan AD, Moore W (2019) Impacts of 21st century climate change on montane habitat in the Madrean Sky Island Archipelago. ed. by K. Feeley. Diversity and Distributions 25: 1625–1638. https://doi.org/10.1111/ddi.12965

Zhang C, Mirarab S (2022) Weighting by gene tree uncertainty improves accuracy of quartet-based species trees. ed. by A. Takahashi. Molecular Biology and Evolution 39: msac215. https://doi.org/10.1093/molbev/msac215

Supplementary materials

Supplementary material 1

Supplementary data is a xslx file with multiple tabs. Each table includes output or results from analysis (.xlsx)
Link: https://doi.org/10.21425/fob.19.181379.suppl1

Supplementary material 2

Supplementary tables S1–S4 and supplementary figures S1–S18 (.pdf)
Link: https://doi.org/10.21425/fob.19.181379.suppl2